



The spatial distribution of multiple elements in the Kanto region of Japan: Transport of chalcophile elements from land to sea



Atsuyuki Ohta*, Noboru Imai, Shigeru Terashima, Yoshiko Tachibana

Geological Survey of Japan, National Institute of Advanced Industrial Science and Technology, Central 7, 1-1-1 Higashi, Tsukuba, Ibaraki 305-8567, Japan

ARTICLE INFO

Article history:

Received 3 December 2013

Revised 19 November 2014

Accepted 24 November 2014

Available online 17 December 2014

Keywords:

Geochemical mapping

Particle transfer

Chalcophile element

Factor analysis

Analysis of variance (ANOVA)

Multiple comparison

ABSTRACT

The transport of particles in the Kanto region of Japan is discussed, using comprehensive geochemical maps of 53 elements in terrestrial and marine areas, generated by the Geological Survey of Japan (AIST). This study investigates the transport processes of elements (Cu, Zn, Mo, As, Cd, Sn, Sb, Hg, Pb, and Bi), the concentrations of which are highly increased as a result of mining and anthropogenic activities. The Kanto region was selected as a study area, because it includes large-scale economic mines, as well as the metropolis of Japan with its associated densely populated and industrial areas. Although metalliferous deposits typically enhance the concentrations of chalcophile elements, and Mo and Sn, marine sediments located adjacent the mining areas show no significant enrichment in these elements. Other elements show that their concentrations are mainly controlled by lithology, and display discontinuous spatial distribution patterns across the land and sea. The coastal sea adjacent to the mining area faces the open sea on the Pacific side. It is, therefore, assumed that sediments supplied from the land would be dispersed by wave and coastal sea currents in the coastal sea environment. In contrast, chalcophile elements, P, Mo, and Sn are highly abundant in both the stream sediments of metropolitan areas and the coastal sea sediments of the adjoining inner Tokyo Bay. The contaminated sediments in the bay appear not to extend into the outer sea. In Tokyo Bay, sea water flows along the bottom from the outer sea towards the inner bay, while surface water in the bay flows out steadily. Accordingly, the spatial distribution patterns of contaminated sediments supplied from the nearby urban areas are controlled by water circulation in the bay.

© 2014 Elsevier B.V. All rights reserved.

1. Introduction

Geochemical maps provide basic information for mineral exploration and environmental assessment, and in this respect many countries have produced national geochemical atlases or collections of regional distribution maps (Andersson et al., 2014; Fauth et al., 1985; Gustavsson et al., 2001; Koljonen, 1992; Lahermo et al., 1990, 1996; Lis and Pasieczna, 1995; Shacklette and Boerngen, 1984; Thalmann et al., 1989; Weaver et al., 1983; Webb et al., 1978; Xie et al., 1997; Zheng, 1994). Darnley et al. (1995) set guidelines for the development of a global geochemical database, and more recently cross-boundary and continental- and sub-continental-scale geochemical mapping projects have been actively conducted (e.g., Bølviken et al., 1986; Caritat and de Cooper, 2011a, 2011b; De Vos, 2006; Reimann et al., 2003, 2014a,b; Salminen et al., 2005; Smith et al., 2013, 2014).

The Geological Survey of Japan, National Institute of Advanced Industrial Science and Technology conducted comprehensive research into the spatial distribution of 53 elements in terrestrial and marine environments during 1999–2008 (Imai et al., 2004, 2010). Japan is surrounded by sea and, therefore, gaining an understanding of the background elemental

abundances in both terrestrial and marine areas is considered important. The production of a comprehensive geochemical atlas, covering the land and the sea, could be used as a powerful tool for examining particle transport processes, particularly the diffusion of pollutants (Ohta and Imai, 2011). However, previous studies in relation to this work have focused mainly on the system of sediment dispersal from terrestrial areas to the coastal sea, in terms of erosion, transport, and deposition of sediments (Ohta et al., 2004, 2007, 2010).

It is also recognised that inner bays often sustain damage from anthropogenic activities from the adjacent terrestrial area. A number of studies have focused on specific areas, such as conducting the environmentally oriented geochemical mapping on soil substances in urbanised areas (Cicchella et al., 2008; Jarva et al., 2008; Johnson and Ander, 2008; Johnson et al., 2011; Li et al., 2004; Thornton et al., 2008). The spatial distribution of pollutants in the marine environment, including within harbours, inner bays, and coastal seas has been examined by Buckley and Winters (1992), Fang et al. (2009), Leoni and Sartori (1996), Li et al. (2001), and Whalley et al. (1999).

However, few comprehensive geochemical surveys have been carried out with respect to anthropogenic activities across both terrestrial and marine environments. Therefore, this study is focused on the Kanto Region of Japan, which includes the metropolis of Japan, highly populated areas, industrial areas, and mining areas, and reveals the transport of

* Corresponding author. Tel.: +81 298 61 3848; fax: +81 298 61 3566.
E-mail address: a.ohta@aist.go.jp (A. Ohta).

chalcophile elements (Cu, Zn, As, Cd, Sb, Hg, Pb, and Bi), Mo, and Sn from terrestrial to marine areas related to mining and anthropogenic activities.

2. Study area

A schematic map of the study area and a land use map with geographical names are shown in Fig. 1a and b, respectively. The Kanto region, is located on the Pacific side of Japan, and has a population of approximately 40 million. It consists of large tracts of flat land, and is an important industrial area that has been affected by pollution, especially during the 1960–1970s. Tokyo Bay, in particular is surrounded by highly populated and industrial areas, and major rivers (the Edo, Ara, and Tama) flow through urban areas to the bay. In addition, the Sagami River flows to Sagami Bay, where the sea floor slopes steeply from the coast and reaches a water depth of 1000 m at a location only 10–20 km offshore. Kashima-Nada is the continental shelf.

Fig. 1c is a 1:1,000,000 scale geological map (Geological Survey of Japan, 1992), which shows that more than half of the study area is covered by Pleistocene–Holocene unconsolidated sediments. Tokyo, Yokohama, Kawasaki, and Chiba cities, each with a population of more than 800,000, are located on coastal plains. The mountainous region is mostly underlain by rocks that formed before the Neogene. The accretionary complexes here consist of mélangé, mudstone, and sandstone, associated with chert, limestone, metabasalt, and ultramafic rock blocks.

Granitic rocks bearing K-feldspar and biotite are distributed in the north-eastern, north-western, and western parts of the study area. The mafic volcanic rocks trend in a NE–SW direction, and are composed of andesitic lava, tuff, and welded tuff. The minor lithologies in the study area are felsic volcanic rocks composed of dacitic lava and tuff, and metamorphic rocks. Fig. 1c also shows the location of some of the major economically mined deposits (Omori et al., 1986). The Hitachi and Ashio mines contain Kieslager-type (Besshi-type) massive sulphide and the vein and massive metasomatic deposits, respectively. These mines are the largest copper mines in Japan. In addition, Takatori mine is a polymetallic W, Sn, Cu, and As deposit. Tochigi mine is a small-scale hydrothermal copper deposit.

3. Sampling locations and sample types

The sampling locations with their respective particle sizes are presented in Fig. 2. In 1980, 65 marine sediment samples were collected using a grab sampler off the Boso Peninsula, and these were subsequently stored in a refrigerating room. In 2004, 125 samples were collected using a grab sampler from Kashima-Nada, Tokyo Bay, and Sagami Bay, with a mean sampling density of one sample per 80 km². The samples were classified into six categories according to their grain size, as determined by visual inspection on board the ship, namely gravel, very coarse–coarse sand, medium sand, fine–very fine sand, sandy silt, and silt. The

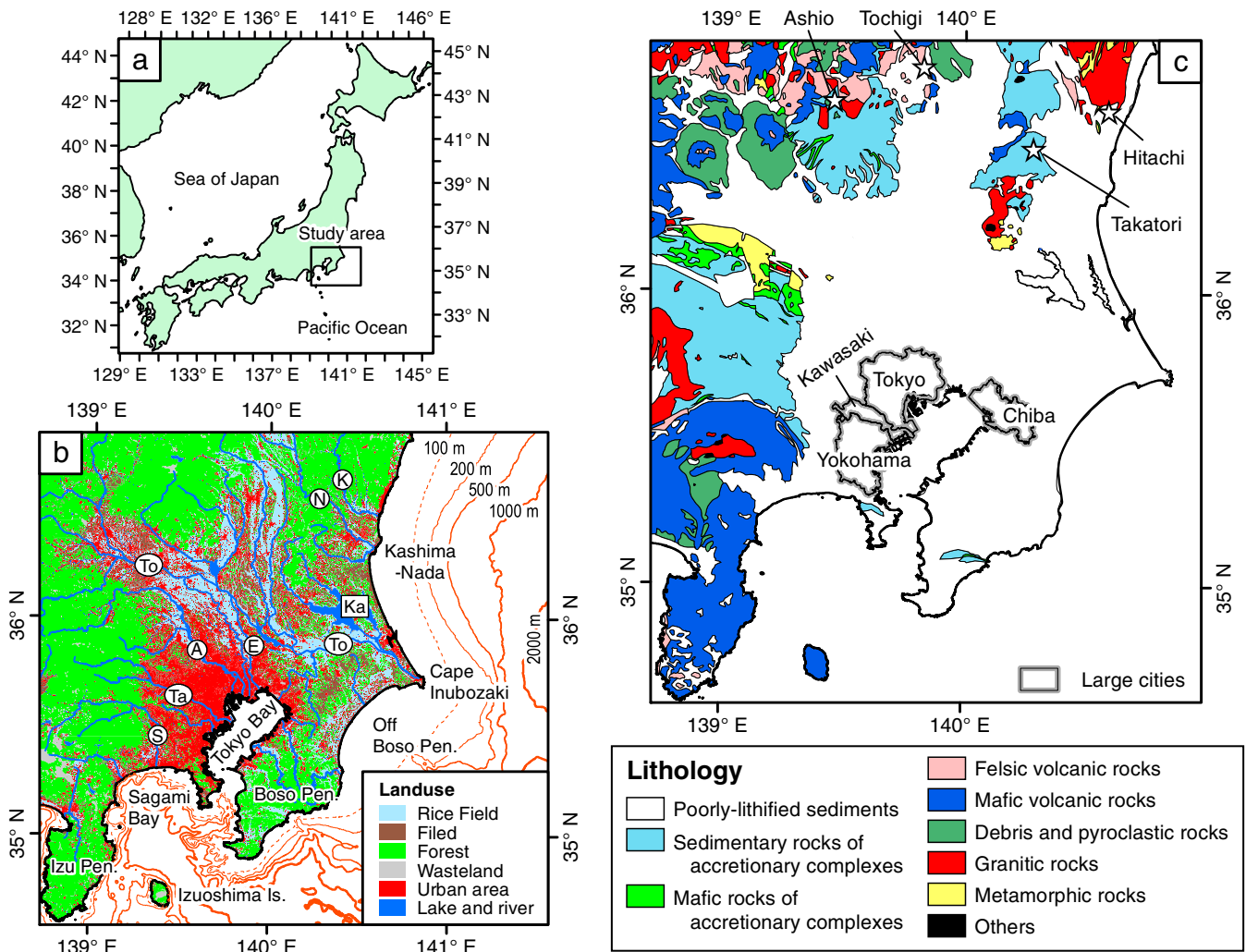


Fig. 1. Schematic maps of the study area: (a) overview map; (b) land use map with geographical names; (c) lithology, major metalliferous mines (indicated by stars) and location of large cities (Geological Survey of Japan, 1992). The abbreviations A, E, Ka, N, Ta, To, and S respectively signify the Ara River, Edo River, Kasumigaura Lake, Naka River, Tama River, Tone River, and Sagami River.

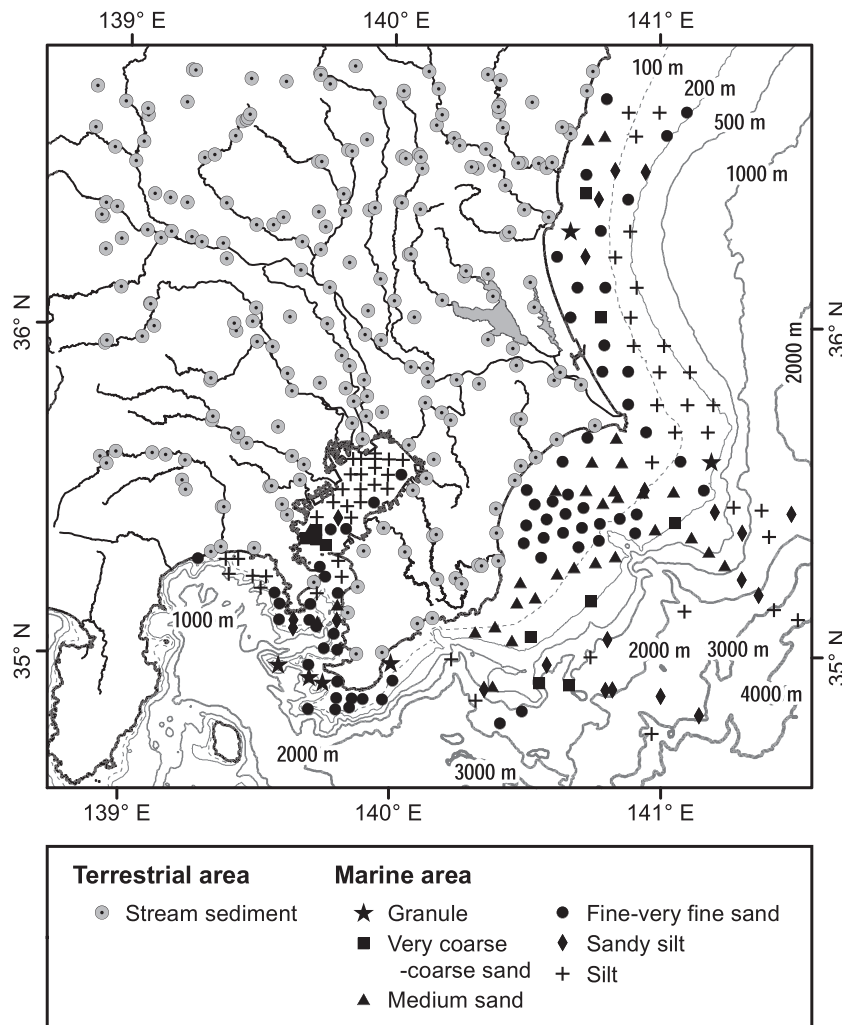


Fig. 2. Sampling locations of stream and marine sediments in the Kanto region, Japan.

uppermost 0–3 cm of the sediments collected with the grab sampler was then separated, air dried, ground with an agate mortar and pestle, and retained for chemical analysis.

Sandy sediments are found distributed widely across the continental shelf, and gravel and coarse sand occur on topographic highs and in the mouth of Tokyo Bay. Silty sediments were found in Tokyo and Sagami Bays at depths of 100–200 m below sea level on the Kashima-Nada shelf, and off the Boso Peninsula in deep sea at depths of over 500 m.

Between 1999 and 2002, 220 stream sediment samples with a mean sampling density of one sample per 100 km² were collected from adjacent terrestrial regions, and these were used for combined geochemical mapping (Imai et al., 2004). The samples were air dried and sieved through an 83 mesh (180 μm) screen. The fine fraction was then retained for analysis, but in contrast to the process used for the marine sediments, these samples were not milled. The sampling locations and their geography, geology, and geochemical background were previously described by Ohta et al. (2011).

4. Analytical methods

The analytical procedure for stream and marine sediments follows the method of Imai (1990). An aliquot of 0.2 g of each sample was digested using a three acid (HF, HNO₃, and HClO₄) digestion at 120 °C for 2 h. The degraded product was then evaporated until dryness at 200 °C, and the residue was dissolved in 100 ml of 0.35 M HNO₃ solution. Element concentrations were determined by ICP–AES for Na, Mg, Al, P, K, Ca, Ti,

Mn, Fe, V, Sr, and Ba, and by ICP–MS for Li, Be, Sc, Cr, Co, Ni, Cu, Zn, Ga, Rb, Zr, Nb, Y, Mo, Cd, Sn, Sb, Cs, La, Ce, Pr, Nd, Sm, Eu, Gd, Tb, Dy, Ho, Er, Tm, Yb, Lu, Hf, Ta, Tl, Pb, Bi, Th, and U. Determination of As and Hg was subcontracted to ALS Chemex (Vancouver, BC), while that within marine sediments was conducted using thermal decomposition, gold amalgamation, and atomic absorption analysis.

For quality control, geochemical reference samples JB-1 and JB-3 (Imai et al., 1995) were inserted every 10 and 20 samples, respectively. Table 1 presents the analytical results obtained for the marine and river sediments, where the major elements (Na, Mg, Al, P, K, Ca, Ti, Mn, and Fe) in sediment are expressed as oxides, because their abundance is frequently expressed in terms of weight per cent oxides. It should be noted that the heavy mineral fraction of the samples, especially zircon, cannot be satisfactorily decomposed by the three-acid (HF, HNO₃, and HClO₄) digestion and, therefore, incomplete decomposition of these minerals seriously affects the concentrations of Zr and Hf. In addition, the marine sediments were not desalinated and, thus, data for Na (Na₂O) in marine sediments and all values for Zr and Hf should be used as a guide only. Hence, from this point onwards Na (Na₂O), Zr, and Hf are excluded from any discussion pertaining to marine sediments.

5. Geochemical map preparation

Terrestrial and marine geochemical maps were prepared using geographical information system (GIS) software (ArcView 10; Environmental Systems Research Institute, Inc. (ESRI)). The Inverse Distance

Table 1
Summary for the geochemistry of marine and stream sediments around Kanto region, Japan.

| Element | Unit | Marine sediments (N = 190) | | | Stream sediments (N = 220) | | |
|----------------------------------|-------|----------------------------|-------|---------------|----------------------------|-------|--------------|
| | | Median | Mean | (min–max) | Median | Mean | (min–max) |
| Na ₂ O | wt.% | 2.68 | 2.82 | (1.18–6.08) | 2.03 | 2.01 | (0.36–3.67) |
| MgO | wt.% | 3.36 | 3.74 | (0.59–8.11) | 3.42 | 3.59 | (0.97–8.32) |
| Al ₂ O ₃ | wt.% | 10.27 | 10.28 | (1.18–15.48) | 10.65 | 10.72 | (6.07–17.45) |
| P ₂ O ₅ | wt.% | 0.106 | 0.113 | (0.022–0.485) | 0.128 | 0.163 | (0.051–1.18) |
| K ₂ O | wt.% | 1.33 | 1.23 | (0.20–1.83) | 1.42 | 1.46 | (0.34–2.85) |
| CaO | wt.% | 4.96 | 7.83 | (0.69–39.9) | 3.07 | 3.17 | (0.46–8.99) |
| TiO ₂ | wt.% | 0.581 | 0.635 | (0.048–2.48) | 0.752 | 0.807 | (0.29–2.46) |
| MnO | wt.% | 0.105 | 0.116 | (0.028–0.33) | 0.132 | 0.149 | (0.053–2.38) |
| T-Fe ₂ O ₃ | wt.% | 6.42 | 6.92 | (0.88–22.1) | 6.77 | 7.05 | (2.52–17.2) |
| Li | mg/kg | 21.9 | 24.4 | (5.49–61.1) | 23.4 | 24.7 | (8.49–115) |
| Be | mg/kg | 0.80 | 0.76 | (0.10–1.36) | 1.01 | 1.16 | (0.33–16.1) |
| Sc | mg/kg | 17.1 | 18.9 | (1.46–45.2) | 16.7 | 18.0 | (4.25–47.2) |
| V | mg/kg | 116 | 135 | (17–561) | 146 | 154 | (42–350) |
| Cr | mg/kg | 40.8 | 47.6 | (8.76–141) | 50.2 | 67.7 | (18.0–469) |
| Co | mg/kg | 14.1 | 15.3 | (1.55–41.3) | 18.4 | 20.1 | (5.44–101) |
| Ni | mg/kg | 17.2 | 20.1 | (6.27–61.0) | 20.8 | 29.8 | (6.44–184) |
| Cu | mg/kg | 18.6 | 29.4 | (2.98–107) | 32.7 | 127 | (6.94–6723) |
| Zn | mg/kg | 86.1 | 110 | (15.7–425) | 113 | 162 | (62–1513) |
| Ga | mg/kg | 12.7 | 12.0 | (1.37–15.8) | 15.2 | 15.2 | (11.5–22.2) |
| As | mg/kg | 6.7 | 8.0 | (1.0–32.1) | 8.0 | 15.8 | (1.0–334) |
| Rb | mg/kg | 31.5 | 31.7 | (2.89–79.2) | 47.8 | 51.8 | (5.89–130) |
| Sr | mg/kg | 223 | 362 | (70–2333) | 144 | 146 | (36–271) |
| Y | mg/kg | 13.9 | 14.1 | (4.22–33.3) | 14.9 | 15.6 | (6.22–29.1) |
| Zr | mg/kg | 38.9 | 38.0 | (4.3–65.6) | 41.2 | 41.5 | (14.5–75) |
| Nb | mg/kg | 3.80 | 3.71 | (0.29–12.4) | 5.55 | 5.86 | (0.88–16.1) |
| Mo | mg/kg | 0.97 | 1.34 | (0.32–8.05) | 1.07 | 1.48 | (0.35–23.0) |
| Cd | mg/kg | 0.09 | 0.19 | (0.016–1.33) | 0.13 | 0.40 | (0.044–28.9) |
| Sn | mg/kg | 1.10 | 1.64 | (0.29–8.34) | 2.21 | 4.45 | (0.94–104) |
| Sb | mg/kg | 0.36 | 0.42 | (0.049–1.39) | 0.54 | 0.98 | (0.089–25.6) |
| Cs | mg/kg | 1.37 | 1.64 | (0.17–5.11) | 2.57 | 2.94 | (0.46–16.8) |
| Ba | mg/kg | 228 | 242 | (22–2031) | 359 | 383 | (88–2915) |
| La | mg/kg | 9.35 | 9.58 | (1.47–34.3) | 14.9 | 16.1 | (2.69–47.3) |
| Ce | mg/kg | 18.8 | 19.5 | (3.2–70.1) | 27.7 | 30.7 | (6.53–91.2) |
| Pr | mg/kg | 2.39 | 2.39 | (0.47–7.59) | 3.49 | 3.75 | (0.95–10.6) |
| Nd | mg/kg | 10.2 | 10.1 | (2.20–29.3) | 14.1 | 15.0 | (4.72–40.7) |
| Sm | mg/kg | 2.33 | 2.29 | (0.65–5.50) | 2.94 | 3.11 | (1.44–7.65) |
| Eu | mg/kg | 0.67 | 0.65 | (0.17–1.02) | 0.74 | 0.77 | (0.42–1.39) |
| Gd | mg/kg | 2.36 | 2.33 | (0.72–4.82) | 2.80 | 2.95 | (1.49–6.17) |
| Tb | mg/kg | 0.43 | 0.43 | (0.12–0.90) | 0.48 | 0.51 | (0.26–0.92) |
| Dy | mg/kg | 2.30 | 2.32 | (0.63–5.31) | 2.52 | 2.63 | (1.33–4.50) |
| Ho | mg/kg | 0.46 | 0.47 | (0.13–1.12) | 0.50 | 0.51 | (0.25–0.88) |
| Er | mg/kg | 1.38 | 1.40 | (0.34–3.41) | 1.47 | 1.51 | (0.64–2.47) |
| Tm | mg/kg | 0.22 | 0.22 | (0.056–0.55) | 0.24 | 0.24 | (0.11–0.37) |
| Yb | mg/kg | 1.40 | 1.41 | (0.31–3.34) | 1.49 | 1.49 | (0.69–2.20) |
| Lu | mg/kg | 0.21 | 0.21 | (0.043–0.50) | 0.22 | 0.22 | (0.094–0.33) |
| Hf | mg/kg | 1.16 | 1.10 | (0.043–1.87) | 1.19 | 1.19 | (0.48–2.08) |
| Ta | mg/kg | 0.35 | 0.34 | (0.12–0.97) | 0.49 | 0.54 | (0.083–5.38) |
| Hg | µg/kg | 70 | 129 | (2–906) | 30 | 52 | (1–540) |
| Tl | mg/kg | 0.26 | 0.31 | (0.010–1.08) | 0.40 | 0.43 | (0.059–3.03) |
| Pb | mg/kg | 14.4 | 18.0 | (4.53–66.7) | 19.4 | 31.8 | (6.37–499) |
| Bi | mg/kg | 0.15 | 0.24 | (0.041–1.41) | 0.15 | 0.50 | (0.029–19.7) |
| Th | mg/kg | 2.98 | 3.07 | (0.26–15.7) | 4.69 | 5.45 | (0.45–26.3) |
| U | mg/kg | 0.84 | 0.92 | (0.29–2.52) | 1.01 | 1.06 | (0.18–3.39) |

Weighting (IDW) method was used for interpolation of point data (Watson and Philip, 1985). In addition, chemical concentrations of stream sediment from a particular sampling site were assumed to represent the average chemical concentrations of the drainage basin upstream (Hawkes, 1957; Hawkes and Webb, 1962; Howarth and Thornton, 1983; Levinson, 1974, 1980; Rose et al., 1979). Thus, terrestrial geochemical maps were generated with a consideration of watersheds (details for this method are given in Ohta et al., 2004). The marine geochemical maps were simply interpolated from data points using the IDW method, and the resultant marine geochemical maps were then combined with the existing land geochemical maps. The class boundaries for concentration intervals follow those of Reimann (2005), i.e., 5, 10, 25, 50, 75, 90, and 95%, and the classification of elemental concentrations was performed for both stream and marine sediments. Figs. 3 and 4 present the comprehensive geochemical maps of 14 elements, including the chalcophile elements (Cu, Zn, As, Cd, Hg and Pb).

6. Results

6.1. Factor analysis of elemental concentrations in stream and marine sediments

To analyse the similarities between elements within the terrestrial and marine geochemical maps, factor analysis was applied to the data sets. Factor analysis requires that the data follow a normal distribution, and geochemical data are assumed to follow either a normal distribution or a lognormal distribution (Ohta et al., 2005), although the validity of these assumptions is presently questioned as geochemical data are compositional data and do not belong to the classical Euclidean space, which is the basis of all classical statistical methods, but define points in the Aitchison geometry on the simplex (Filzmoser et al., 2014). Consequently, they need to be considered in their own Euclidean geometry on the simplex (Aitchison, 1986; Filzmoser et al., 2009, 2010; Egozcue and Pawlowsky-Glahn, 2011; Reimann et al., 2012; Buccianti, in this

issue; Sadeghi et al., in this issue). However, in this study the hitherto assumptions of normal or lognormal data distribution are followed. Therefore, the Shapiro–Wilk test was firstly conducted to examine the normality of elemental concentrations (Shapiro and Wilk, 1965) (Table 2). In this test, it is assumed that the data followed a normal distribution when the probability exceeds 0.05. However, Table 2 shows that most of the data follow neither a normal nor a lognormal distribution and, therefore, a data symmetry approach was considered the second best alternative for use (e.g., Ohta et al., 2005). Consequently, a data distribution with a skewness closer to zero was used for the statistical test. Finally, the data of 41 elements for stream sediments and those of 30 elements for marine sediment were log-transformed; the other data remained unchanged (Table 2).

Factor analysis was conducted using the Varimax orthogonal rotation procedure on (Table 3). In order to reduce the number of variables, La and Yb were selected from the lanthanides. However, there were not enough samples (220 stream sediment samples and 190 marine sediment samples) to obtain stable results from a factor analysis for 39 variables (Reimann et al., 2002) and, therefore, the calculated results can only be used as a guide. Table 3 shows that similar results were obtained for both the stream and marine sediment data sets. The fifth factor is excluded here, because its contribution is smaller than 5% of the total variance for stream and marine sediments.

Factor 1 has high positive loadings on alkali elements, Be, Nb, Ba, La, Ta, Tl, Th, and U, and negative loadings on CaO (group 1) for stream and marine sediments. This factor reflects the contribution from granitic

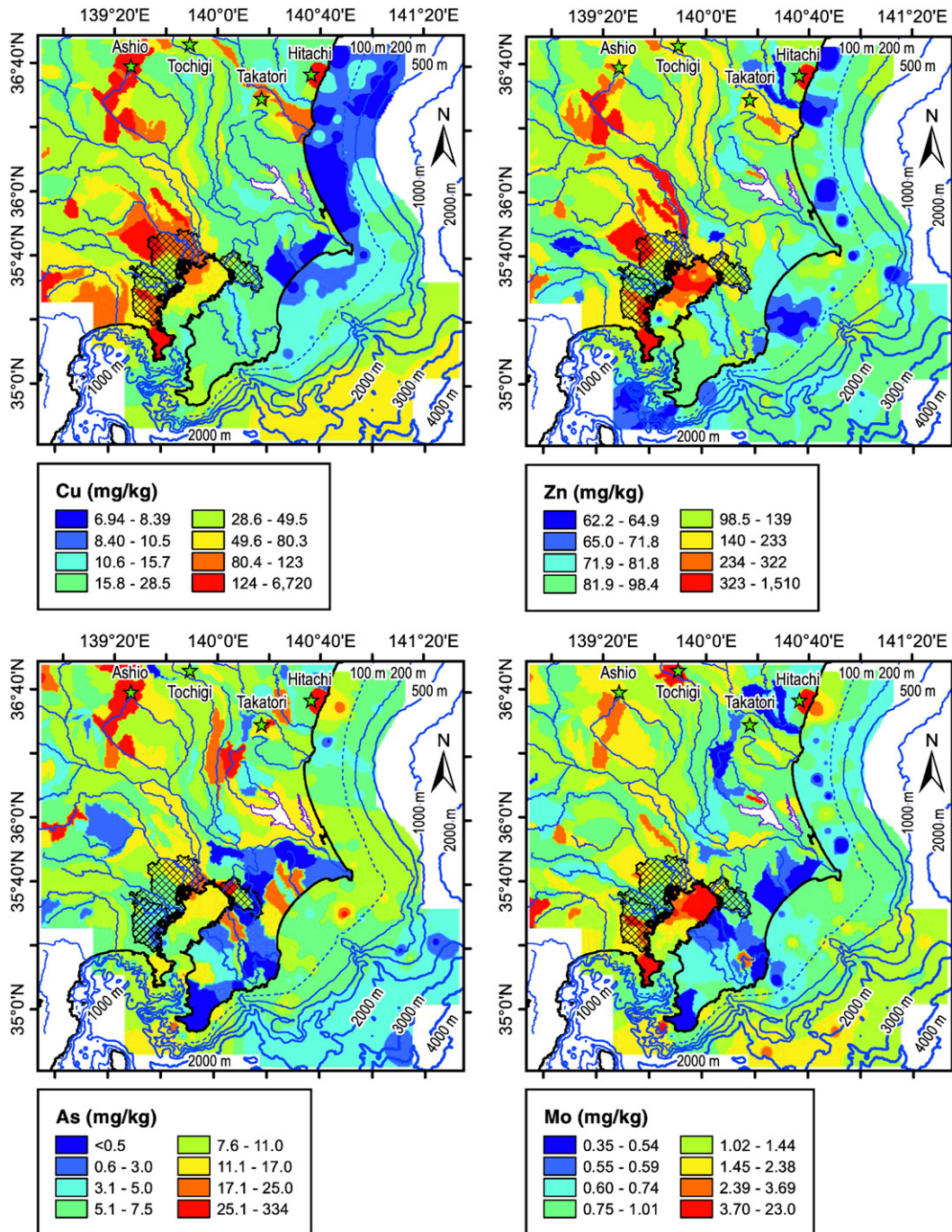


Fig. 3. Spatial distribution of elemental concentrations in stream sediments for six chalcophile elements, and Mo and Sn. Class selection grouped according to percentiles (5, 10, 25, 50, 75, 90, 95, and 100%) for stream and marine sediments (see text). Large star symbols represent mineral deposits.

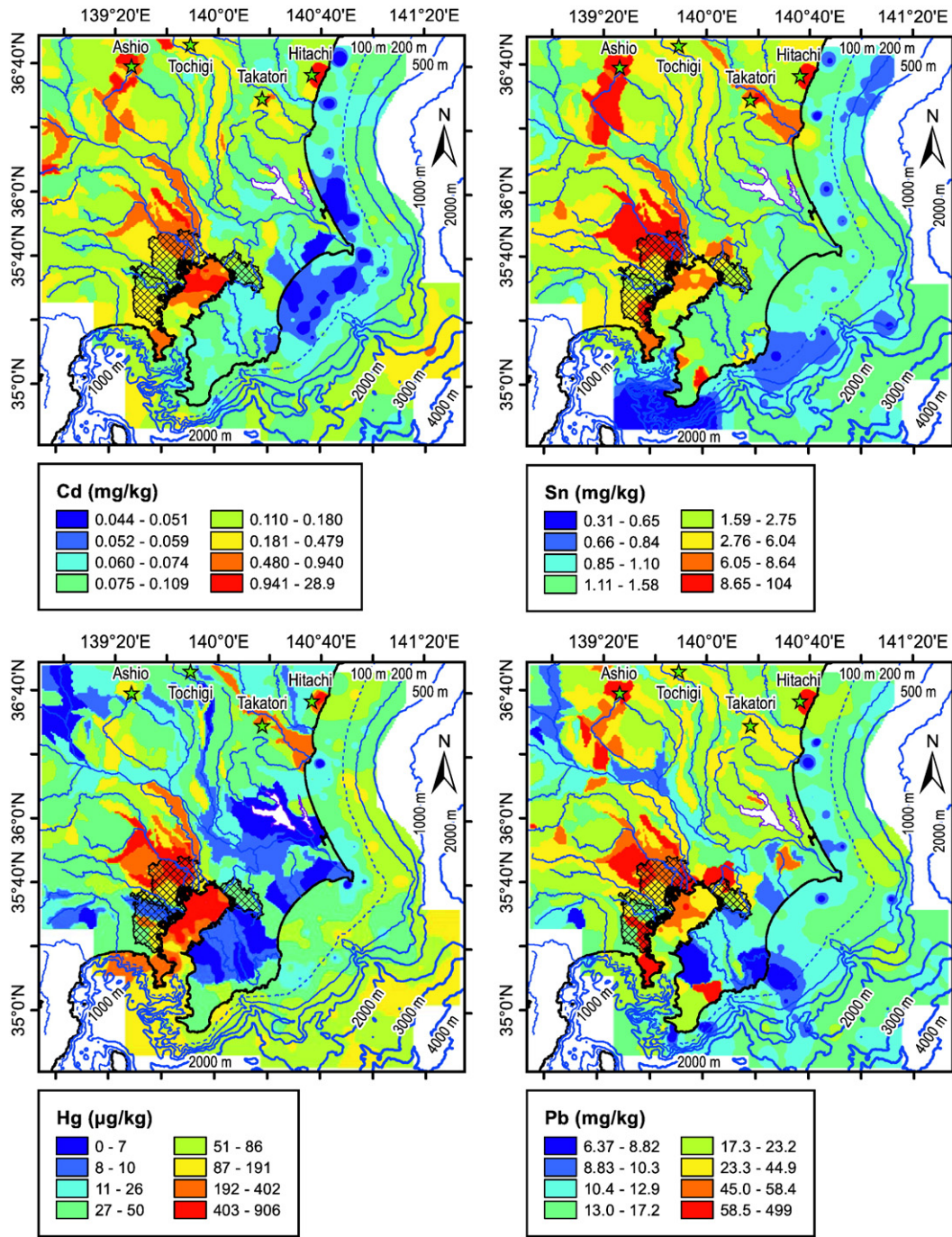


Fig. 3 (continued).

rocks and felsic volcanic rocks in the terrestrial area. Factor 2 has high positive loadings on P_2O_5 , Cr, Ni, Cu, Zn, As, Mo, Cd, Sn, Sb, Cs, Hg, Pb, and Bi (group 2) in stream and marine sediments, and may thus indicate metalliferous deposits and contamination in both the terrestrial and marine environment. Factor 3 is controlled by MgO, Sc, TiO_2 , V, MnO, T- Fe_2O_3 (total), and Co for stream and marine sediments (group 3), and this suggests the contribution of mafic volcanic rocks. It is noted that Y and Yb are included in Factor 3 for stream sediments, but are classified as Factor 4 for marine sediments. In contrast, Factor 4 of the stream sediments reflects the association of Na_2O , Al_2O_3 , CaO, Ga, and Sr and indicates the abundance of plagioclase in stream sediments. In the following sections, the differences between the terrestrial and marine environments are elucidated with respect to the spatial distribution patterns within each group.

6.2. Spatial distribution patterns of chalcophile elements and Mo and Sn, in both the terrestrial and marine environments

Chalcophile elements include Cu, Zn, As, Cd, Sb, Hg, Pb, and Bi, as well as Mo and Sn, although the latter two also have siderophile affinities, and are classified as group 2 in both the stream and the marine sediment data sets (Table 3). In the terrestrial area, these elements are highly enriched around mineral deposits, such as those within the Ashio, Takatori, and Hitachi mines, and in urban area (Fig. 3a and b). The Japanese geochemical mapping project avoided collecting visibly polluted sediments from urban areas, because the aim of the project was to obtain natural background levels of 53 elements across Japan. Nevertheless, significant enrichment of nine elements (P_2O_5 , Cr, Ni, Cu, Zn, Sn, Sb, Hg, and Pb) was statistically confirmed in urban areas (Ohta et al.,

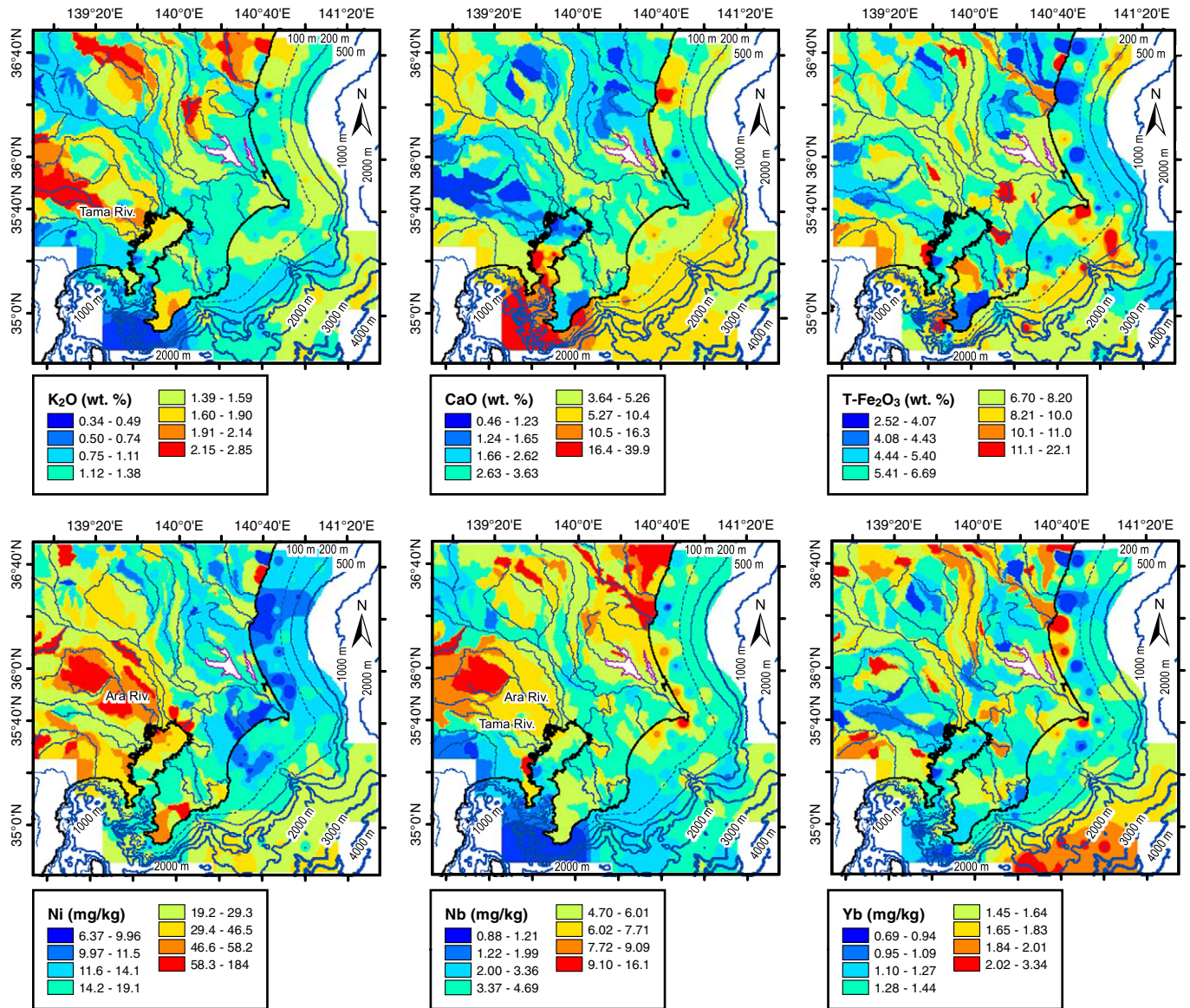


Fig. 4. Spatial distribution of elemental concentrations in stream and marine sediments for K₂O, CaO, T-Fe₂O₃, Ni, Nb, and Yb. Class selection is the same as in Fig. 3.

2011). In addition, coastal sea sediments from the closed-off section of Tokyo Bay, which is surrounded by highly-populated areas and industrial zones, also tended to be rich in chalcophile elements, P₂O₅, Cr, Ni, Mo, and Sn. The enrichment of these elements is considered likely to have been caused by the input of sediments related to anthropogenic activities. However, the concentration of these elements is lower in the outer part of Tokyo Bay, which is covered by coarse sands (Fig. 2). Elsewhere, mineral occurrences (such as those at Hitachi, Ashio, and Takatori mines) strongly affect the abundance of chalcophile elements, Mo, and Sn in stream sediments, although these elemental enrichments seem to be limited to a small area. Stream sediments collected from the drainage basins downstream from the Takatori and Hitachi mines contained 2000–6700 mg/kg of Cu, 1000–1500 mg/kg of Zn, 7–23 mg/kg of Mo, 6–29 mg/kg of Cd, 25–104 mg/kg of Sn, ~25 mg/kg of Sb, and 5–12 mg/kg of Bi. The highest amounts of these elemental concentrations in all stream sediment samples collected across the whole of Japan. However, marine sediments, located near the estuaries of the rivers flowing through Hitachi and Takatori mines, were not found to be enriched in chalcophile elements, although there was an exception to this, namely the coastal sea sediments retrieved offshore from the Hitachi mine were found to have high As and Mo concentrations.

6.3. Spatial distribution of elements controlled by surface lithology

The spatial distribution of most elemental concentrations in terrestrial areas is controlled simply by surface lithology (Ohta et al., 2011). In the study area, stream sediments collected from rivers over granitic rocks were found to be highly enriched in Be, Na₂O, K₂O, Ga, Nb, rare earth elements (REEs: Y and lanthanide), Ta, Th, and U (represented by Nb and Yb in Fig. 4). Concentrations of Li, Be, K₂O, Rb, Cs, Ba, and Tl were found to be elevated in regions where sedimentary rocks in accretionary complexes and felsic volcanic rocks outcrop (represented by K₂O in Fig. 4). Because granitic rocks, felsic volcanic rocks, and sedimentary rocks in accretionary complexes are situated at close proximity to each other in the north, north-west, and west of the study area, these elements are dominantly associated in group 1 of factor analysis. The oxides and elements of MgO, Al₂O₃, P₂O₅, CaO, Sc, TiO₂, V, MnO, T-Fe₂O₃, Co, and Sr (group 3) were found to be abundant in stream sediments derived from mafic volcanic rocks (represented by T-Fe₂O₃ in Fig. 4). However, sediments from mafic-ultramafic rocks in the accretionary complexes, which outcrop in the upper part of the Tama River, the south part of the Boso Peninsular, and around Hitachi mine, were extremely enriched in Cr and Ni (represented by Ni map in Fig. 4).

Table 2Significance probabilities (*p*) of Shapiro–Wilk (*S–W*) test and the skewness applied to marine and stream sediments.

| | Marine sediment | | | | | Stream sediment | | | | |
|----------------------------------|-----------------|-------------|-------|-------|---------------------|-----------------|-------------|-------|-------|---------------------|
| | S–W test | | Skew | | Data transformation | S–W test | | Skew | | Data transformation |
| | Raw | Log | Raw | Log | | Raw | Log | Raw | Log | |
| Na ₂ O | N.D. | N.D. | N.D. | N.D. | N.D. | <0.01 | <0.01 | –0.26 | –2.21 | Unchanged |
| MgO | <0.01 | <0.01 | 0.92 | –0.65 | Log-transformed | <0.01 | 0.58 | 0.74 | –0.19 | Log-transformed |
| Al ₂ O ₃ | <0.01 | <0.01 | –0.43 | –2.57 | Unchanged | 0.08 | 0.61 | 0.38 | –0.18 | Log-transformed |
| P ₂ O ₅ | <0.01 | <0.01 | 2.98 | 0.11 | Log-transformed | <0.01 | <0.01 | 4.22 | 0.89 | Log-transformed |
| K ₂ O | <0.01 | <0.01 | –0.97 | –1.95 | Unchanged | 0.11 | <0.01 | 0.25 | –1.06 | Unchanged |
| CaO | <0.01 | <0.01 | 2.26 | 0.31 | Log-transformed | <0.01 | <0.01 | 0.73 | –0.86 | Unchanged |
| TiO ₂ | <0.01 | <0.01 | 2.42 | –1.36 | Log-transformed | <0.01 | <0.01 | 2.27 | 0.50 | Log-transformed |
| MnO | <0.01 | 0.48 | 1.08 | –0.03 | Log-transformed | <0.01 | <0.01 | 13.08 | 1.88 | Log-transformed |
| T-Fe ₂ O ₃ | <0.01 | <0.01 | 1.34 | –1.18 | Log-transformed | <0.01 | 0.84 | 1.13 | 0.002 | Log-transformed |
| Li | <0.01 | <0.01 | 1.20 | –0.13 | Log-transformed | <0.01 | <0.01 | 3.86 | 0.32 | Log-transformed |
| Be | <0.01 | <0.01 | –0.70 | –1.92 | Unchanged | <0.01 | <0.01 | 11.73 | 1.52 | Log-transformed |
| Sc | <0.01 | <0.01 | 0.71 | –1.19 | Unchanged | <0.01 | 0.46 | 1.03 | –0.25 | Log-transformed |
| V | <0.01 | <0.01 | 2.12 | –0.33 | Log-transformed | <0.01 | 0.76 | 0.96 | –0.09 | Log-transformed |
| Cr | <0.01 | <0.01 | 1.78 | 0.07 | Log-transformed | <0.01 | <0.01 | 4.38 | 1.22 | Log-transformed |
| Co | <0.01 | <0.01 | 0.89 | –0.83 | Log-transformed | <0.01 | <0.01 | 3.61 | 0.46 | Log-transformed |
| Ni | <0.01 | <0.01 | 1.59 | 0.54 | Log-transformed | <0.01 | <0.01 | 2.88 | 0.81 | Log-transformed |
| Cu | <0.01 | <0.01 | 1.16 | 0.16 | Log-transformed | <0.01 | <0.01 | 8.92 | 2.13 | Log-transformed |
| Zn | <0.01 | <0.01 | 2.52 | 0.82 | Log-transformed | <0.01 | <0.01 | 5.36 | 1.81 | Log-transformed |
| Ga | <0.01 | <0.01 | –1.81 | –3.72 | Unchanged | <0.01 | 0.25 | 0.46 | 0.09 | Log-transformed |
| As | <0.01 | <0.01 | 1.59 | –1.27 | Log-transformed | <0.01 | <0.01 | 6.03 | 0.36 | Log-transformed |
| Rb | 0.04 | <0.01 | 0.19 | –1.75 | Unchanged | <0.01 | <0.01 | 0.61 | –1.00 | Unchanged |
| Sr | <0.01 | <0.01 | 3.08 | 0.96 | Log-transformed | 0.06 | <0.01 | 0.35 | –0.68 | Unchanged |
| Y | <0.01 | <0.01 | 1.00 | –1.16 | Unchanged | <0.01 | <0.01 | 0.54 | –0.38 | Log-transformed |
| Nb | <0.01 | <0.01 | 0.63 | –1.29 | Unchanged | <0.01 | <0.01 | 1.21 | –0.69 | Log-transformed |
| Mo | <0.01 | <0.01 | 3.01 | 1.28 | Log-transformed | <0.01 | <0.01 | 7.60 | 1.32 | Log-transformed |
| Cd | <0.01 | <0.01 | 2.84 | 1.41 | Log-transformed | <0.01 | <0.01 | 12.87 | 2.29 | Log-transformed |
| Sn | <0.01 | <0.01 | 2.47 | 1.07 | Log-transformed | <0.01 | <0.01 | 7.61 | 1.67 | Log-transformed |
| Sb | <0.01 | <0.01 | 1.79 | –0.15 | Log-transformed | <0.01 | <0.01 | 8.92 | 1.52 | Log-transformed |
| Cs | <0.01 | <0.01 | 1.40 | –0.54 | Log-transformed | <0.01 | 0.26 | 2.93 | 0.08 | Log-transformed |
| Ba | <0.01 | <0.01 | 6.84 | –0.73 | Log-transformed | <0.01 | <0.01 | 7.87 | 0.43 | Log-transformed |
| La | <0.01 | <0.01 | 1.52 | –1.13 | Log-transformed | <0.01 | 0.01 | 1.24 | –0.42 | Log-transformed |
| Ce | <0.01 | <0.01 | 1.66 | –1.11 | Log-transformed | <0.01 | 0.40 | 1.45 | –0.05 | Log-transformed |
| Pr | <0.01 | <0.01 | 1.25 | –1.19 | Log-transformed | <0.01 | 0.74 | 1.40 | –0.02 | Log-transformed |
| Nd | <0.01 | <0.01 | 1.10 | –1.2 | Unchanged | <0.01 | 0.28 | 1.50 | 0.21 | Log-transformed |
| Sm | <0.01 | <0.01 | 0.59 | –1.35 | Unchanged | <0.01 | <0.01 | 1.68 | 0.56 | Log-transformed |
| Eu | <0.01 | <0.01 | –0.89 | –2.55 | Unchanged | <0.01 | <0.01 | 1.04 | 0.26 | Log-transformed |
| Gd | <0.01 | <0.01 | 0.41 | –1.43 | Unchanged | <0.01 | <0.01 | 1.35 | 0.47 | Log-transformed |
| Tb | <0.01 | <0.01 | 0.37 | –1.57 | Unchanged | <0.01 | 0.02 | 1.03 | 0.28 | Log-transformed |
| Dy | <0.01 | <0.01 | 0.74 | –1.46 | Unchanged | <0.01 | 0.04 | 0.63 | –0.13 | Log-transformed |
| Ho | <0.01 | <0.01 | 0.99 | –1.42 | Unchanged | <0.01 | <0.01 | 0.38 | –0.42 | Unchanged |
| Er | <0.01 | <0.01 | 1.08 | –1.42 | Unchanged | 0.15 | <0.01 | 0.20 | –0.62 | Unchanged |
| Tm | <0.01 | <0.01 | 1.09 | –1.38 | Unchanged | 0.56 | <0.01 | 0.01 | –0.75 | Unchanged |
| Yb | <0.01 | <0.01 | 1.00 | –1.52 | Unchanged | 0.47 | <0.01 | –0.08 | –0.78 | Unchanged |
| Lu | <0.01 | <0.01 | 0.98 | –1.58 | Unchanged | 0.74 | <0.01 | –0.09 | –0.82 | Unchanged |
| Ta | 0.02 | <0.01 | 0.20 | –2.05 | Unchanged | <0.01 | <0.01 | 9.15 | 0.03 | Log-transformed |
| Hg | <0.01 | <0.01 | 2.31 | –0.08 | Log-transformed | <0.01 | <0.01 | 3.92 | –1.00 | Log-transformed |
| Tl | <0.01 | <0.01 | 1.66 | –0.96 | Log-transformed | <0.01 | <0.01 | 5.21 | –0.22 | Log-transformed |
| Pb | <0.01 | <0.01 | 2.24 | 0.81 | Log-transformed | <0.01 | <0.01 | 6.33 | 1.66 | Log-transformed |
| Bi | <0.01 | <0.01 | 2.64 | 1.00 | Log-transformed | <0.01 | <0.01 | 7.65 | 1.74 | Log-transformed |
| Th | <0.01 | <0.01 | 2.71 | –1.40 | Log-transformed | <0.01 | <0.01 | 2.65 | –0.51 | Log-transformed |
| U | <0.01 | 0.17 | 1.56 | 0.27 | Log-transformed | <0.01 | <0.01 | 1.40 | –0.63 | Log-transformed |

A bold-faced type means that the null hypothesis is rejected for *p* = 0.05.

N.D.: not determined.

Silty sediments distributed through the inner part of Tokyo Bay are highly enriched in Li, K₂O, Rb, Nb, Cs, Ta, and Tl. It is considered that the elevated concentrations of these elements are likely to be related to the input of lithic fragments and clay minerals from the Tama River. This is because the muddy sediments are derived from an accretionary complex rich in Li, K₂O, Rb, Nb, Cs, Ta, and Tl, which outcrops in the upper part of the Tama River. Similarly, the high concentrations of Al₂O₃, T-Fe₂O₃, Co, and Cu in Sagami Bay reflect the input of sediments originating from mafic volcanic rocks. These spatial features suggest that particles are transported from terrestrial areas via rivers to the coastal sea environment. However, these characteristic distributions are not recognised on the Kashima-Nada shelf and off the Boso Peninsula, and the spatial distribution patterns of elemental concentrations in these regions seem to be

patchy and irregular. Generally, the elemental concentrations tend to increase with increasing water depth. In contrast, CaO and Sr are abundant in sandy sediments and gravels that are distributed on the continental shelf, topographic highs, and in the mouth of Tokyo Bay (see CaO in Fig. 4). Factor analysis suggests that CaO and Sr in marine sediments have strong negative loading for Factor 1 (Table 3). The dilution effect by calcareous materials (such as shell fragments) is considered to be an additional factor. Sandy sediments and sandy silt found off the Boso Peninsula in deep sea at depths of over 500 m are highly enriched in heavy REEs (Y and Gd–Lu) (see Yb in Fig. 4). This is the reason why Y and Yb are included in Factor 3 for stream sediments, but are classified as Factor 4 for marine sediments in factor analysis (Table 3). However, it is unclear what this classification for marine sediments implies.

Table 3
Factor loadings of a factor analysis carried out with 39 variables for marine sediments and 40 variables for stream sediments.

| Element | Marine sediments | | | | | Stream sediments | | | | |
|----------------------------------|------------------|---------------|-------------|-------------|-------------|------------------|---------------|-------------|-------------|-------------|
| | Comm. | Factor 1 | Factor 2 | Factor 3 | Factor 4 | Comm. | Factor 1 | Factor 2 | Factor 3 | Factor 4 |
| Na ₂ O | | | | | | 0.52 | −0.04 | −0.39 | −0.18 | 0.57 |
| MgO | 0.75 | −0.33 | 0.02 | 0.80 | 0.03 | 0.71 | −0.38 | −0.13 | 0.73 | 0.14 |
| Al ₂ O ₃ | 0.70 | −0.04 | 0.04 | 0.40 | 0.74 | 0.64 | −0.32 | 0.00 | 0.24 | 0.69 |
| P ₂ O ₅ | 0.71 | −0.22 | 0.80 | 0.15 | 0.07 | 0.28 | 0.00 | 0.51 | 0.14 | 0.07 |
| K ₂ O | 0.91 | 0.85 | 0.20 | −0.35 | 0.19 | 0.81 | 0.77 | −0.06 | −0.47 | 0.04 |
| CaO | 0.74 | − 0.83 | −0.17 | 0.11 | 0.10 | 0.78 | − 0.61 | −0.14 | 0.37 | 0.51 |
| TiO ₂ | 0.89 | 0.36 | 0.00 | 0.84 | 0.24 | 0.75 | 0.06 | −0.14 | 0.84 | −0.16 |
| MnO | 0.73 | −0.17 | −0.01 | 0.83 | −0.02 | 0.88 | −0.35 | 0.23 | 0.84 | 0.01 |
| T-Fe ₂ O ₃ | 0.84 | 0.01 | 0.02 | 0.90 | 0.17 | 0.46 | −0.05 | 0.25 | 0.63 | 0.00 |
| Li | 0.86 | 0.68 | 0.61 | −0.18 | 0.06 | 0.63 | 0.71 | 0.28 | −0.16 | 0.14 |
| Be | 0.92 | 0.87 | 0.27 | −0.26 | 0.17 | 0.76 | 0.78 | 0.29 | −0.25 | 0.07 |
| Sc | 0.93 | −0.26 | −0.17 | 0.88 | 0.24 | 0.89 | −0.44 | −0.09 | 0.80 | 0.23 |
| V | 0.88 | −0.06 | 0.08 | 0.87 | 0.33 | 0.75 | −0.34 | 0.12 | 0.79 | −0.01 |
| Cr | 0.73 | 0.35 | 0.64 | 0.44 | −0.05 | 0.38 | 0.04 | 0.32 | 0.50 | 0.17 |
| Co | 0.93 | −0.10 | 0.17 | 0.94 | 0.12 | 0.85 | −0.29 | 0.37 | 0.79 | 0.07 |
| Ni | 0.76 | 0.08 | 0.83 | 0.26 | 0.06 | 0.42 | 0.01 | 0.49 | 0.40 | 0.12 |
| Cu | 0.92 | −0.08 | 0.84 | 0.16 | 0.42 | 0.85 | −0.04 | 0.90 | 0.19 | 0.08 |
| Zn | 0.90 | 0.39 | 0.78 | 0.36 | −0.11 | 0.85 | 0.01 | 0.88 | 0.26 | −0.06 |
| Ga | 0.85 | 0.59 | 0.28 | 0.31 | 0.57 | 0.48 | 0.18 | 0.25 | 0.13 | 0.61 |
| As | 0.21 | 0.08 | 0.35 | 0.10 | −0.26 | 0.46 | 0.25 | 0.62 | −0.11 | 0.11 |
| Rb | 0.74 | 0.72 | 0.40 | −0.24 | −0.03 | 0.76 | 0.78 | 0.06 | −0.38 | 0.02 |
| Sr | 0.72 | − 0.84 | −0.13 | −0.02 | −0.01 | 0.73 | −0.34 | −0.16 | 0.02 | 0.76 |
| Y | 0.68 | 0.20 | 0.09 | 0.41 | 0.69 | 0.68 | 0.26 | 0.18 | 0.56 | 0.51 |
| Nb | 0.74 | 0.85 | 0.07 | 0.13 | −0.03 | 0.70 | 0.83 | 0.02 | 0.08 | −0.11 |
| Mo | 0.61 | 0.10 | 0.78 | 0.01 | −0.01 | 0.68 | −0.08 | 0.78 | 0.24 | −0.04 |
| Cd | 0.81 | 0.12 | 0.89 | −0.05 | −0.06 | 0.84 | 0.13 | 0.90 | 0.10 | 0.05 |
| Sn | 0.85 | 0.51 | 0.76 | −0.09 | 0.00 | 0.73 | 0.25 | 0.80 | 0.04 | −0.13 |
| Sb | 0.62 | 0.29 | 0.69 | 0.01 | 0.22 | 0.77 | 0.22 | 0.84 | −0.03 | −0.09 |
| Cs | 0.90 | 0.67 | 0.60 | −0.20 | 0.22 | 0.73 | 0.69 | 0.43 | −0.24 | 0.05 |
| Ba | 0.75 | 0.75 | −0.11 | −0.14 | 0.39 | 0.59 | 0.59 | 0.31 | −0.34 | −0.18 |
| La | 0.77 | 0.87 | −0.06 | 0.12 | −0.03 | 0.79 | 0.88 | 0.00 | 0.05 | −0.12 |
| Yb | 0.76 | 0.27 | −0.01 | 0.42 | 0.71 | 0.58 | 0.07 | 0.06 | 0.62 | 0.43 |
| Ta | 0.76 | 0.83 | 0.24 | 0.11 | 0.08 | 0.40 | 0.59 | 0.20 | 0.09 | 0.00 |
| Hg | 0.75 | −0.02 | 0.84 | −0.20 | 0.02 | 0.50 | 0.34 | 0.61 | −0.05 | −0.09 |
| Tl | 0.85 | 0.77 | 0.42 | −0.28 | 0.03 | 0.87 | 0.72 | 0.50 | −0.30 | −0.11 |
| Pb | 0.80 | 0.28 | 0.83 | −0.08 | −0.15 | 0.65 | 0.21 | 0.76 | −0.03 | −0.14 |
| Bi | 0.88 | 0.34 | 0.87 | −0.12 | 0.03 | 0.74 | 0.27 | 0.82 | 0.00 | 0.00 |
| Th | 0.85 | 0.92 | −0.01 | 0.05 | 0.06 | 0.84 | 0.90 | −0.07 | −0.07 | −0.13 |
| U | 0.50 | 0.47 | 0.47 | −0.16 | 0.17 | 0.75 | 0.82 | 0.21 | −0.07 | −0.13 |
| Eigenvalue | | 10.4 | 9.5 | 6.9 | 2.8 | | 8.7 | 8.4 | 6.5 | 2.8 |
| Variance (%) | | 27 | 25 | 18 | 7 | | 22 | 21 | 17 | 7 |
| Cum. variance (%) | | 27 | 52 | 70 | 78 | | 22 | 43 | 60 | 67 |

Comm.: communality, Cum.: cumulative.

Bold faced type means that the factor loading is larger than 0.5 or smaller than 0.5.

7. Discussion

7.1. Analysis of particle transport in sediment highly enriched in chalcophile elements in relation to mining activity

Despite extremely high concentrations of chalcophile elements, Mo, and Sn, around the Hitachi and Takatori mines, no significant enrichment of these elements was observed in the adjacent marine environments, except for isolated cases of As and Mo. To investigate further, therefore, it was attempted to trace the particle transfer from land to Kashima-Nada along the Pacific coast, using the spatial distribution patterns of non-chalcophile elements.

High concentrations of Cr and Ni were found around the Hitachi mine in relation to small-scale serpentine outcrops occurring within ultramafic rock blocks of the accretionary complex. Serpentine delivers very fine particles to the river systems and, therefore, the spatial distribution patterns of Cr and Ni associated with serpentine can be used as tracers of fine particles (Ohta et al., 2004). Fig. 4 shows that the marine sediments, adjacent to the terrestrial area around the Hitachi mine, lack any enrichment of Cr and Ni, and in contrast, Y, Nb, Ln, Ta, Th, and U are abundant around the Hitachi and Takatori mines. Elements in the sediments of the Kanto Region originate from granitic and sedimentary rocks (dominantly sandstones) in accretionary complexes (Fig. 1c), and are associated with

heavy minerals, such as sphene, monazite, and zircon which have a high specific gravity (e.g., Chandrajith et al., 2000, 2001). However, despite such common characteristics the spatial distribution of these elements is discontinuous across land and sea (represented by Nb in Fig. 4).

The river flowing through the mineralisation zone of the Hitachi mine is only about 10 km long. As such, the discontinuous distribution patterns of chalcophile elements across the land and sea can be attributed, in part, to the small discharge of sediments from rivers. As an alternative explanation, the continental shelf of Kashima-Nada, particularly at shallower water depths of 100 m or less, is dominantly covered by sandy sediments (whereas gravels and coarse sands are deposited patchily), and the coastal area of Kashima-Nada is strongly eroded by waves and strong coastal sea currents (Mogi, 1970; Kubo, 1989). Coastal sea sediments enriched in Y, Nb, Ln, Ta, Th, and U are not found on the Kashima-Nada shelf, but occur instead to the south around Cape Inubo. Aoyama et al. (2012) reported that the coastal sea currents on Kashima-Nada flow anticlockwise (southward), based on data from ¹³⁴Cs and ¹³⁷Cs discharged from the Fukushima Dai-ichi Nuclear Power Plant. From this, it may be supposed that modern sediments supplied by rivers are dispersed by wave and coastal sea currents, and are partly carried southward, thereby resulting in the discontinuous spatial distribution patterns of all elements, including the chalcophile elements, across land and sea.

However, high concentrations of As and Mo were found offshore adjacent to the Hitachi mine (Fig. 3a), and these marine samples also had high T-Fe₂O₃/TiO₂ ratios of 25 and 44. As demonstrated above, particles associated with mines are not expected to be transported directly to the adjacent offshore region, and Fe hydroxides coating coarse grains would be able to adsorb elements supplied from mines as dissolved phases, thus carrying them in the articulate fraction. In addition, one marine sediment sample had a somewhat enriched concentration of Sn (see Sn in Fig. 3b), and this was sampled directly at the mouth of the Naka River (which flows through the metalliferous zone around the Takatori mine). This suggests that tin ore (SnO₂) may remain in situ without being dispersed by waves or currents.

7.2. Behaviour of contaminated sediments in semi-closed Tokyo Bay

The closed-off section of Tokyo Bay is covered by silty sediments highly enriched in chalcophile elements, P₂O₅, Cr, Ni, Mo, and Sn. In contrast, the entrance to the Bay is covered by coarse sands that are poor in these elements, because of the dilution effect related to quartz and shell fragments. The spatial distribution of silt and coarse sand is determined by the water circulation within the bay. Higashi and Maki (2008) suggested that dense sea water, having high salinity, flows from the outer sea to the Bay along the sea floor. In contrast, surface water with low salinity and low density (due to the input of river water) flows from the bay to the outer sea in the upper part of the water column. The speed of the tidal current in the mouth of Tokyo Bay is very high, because it funnels

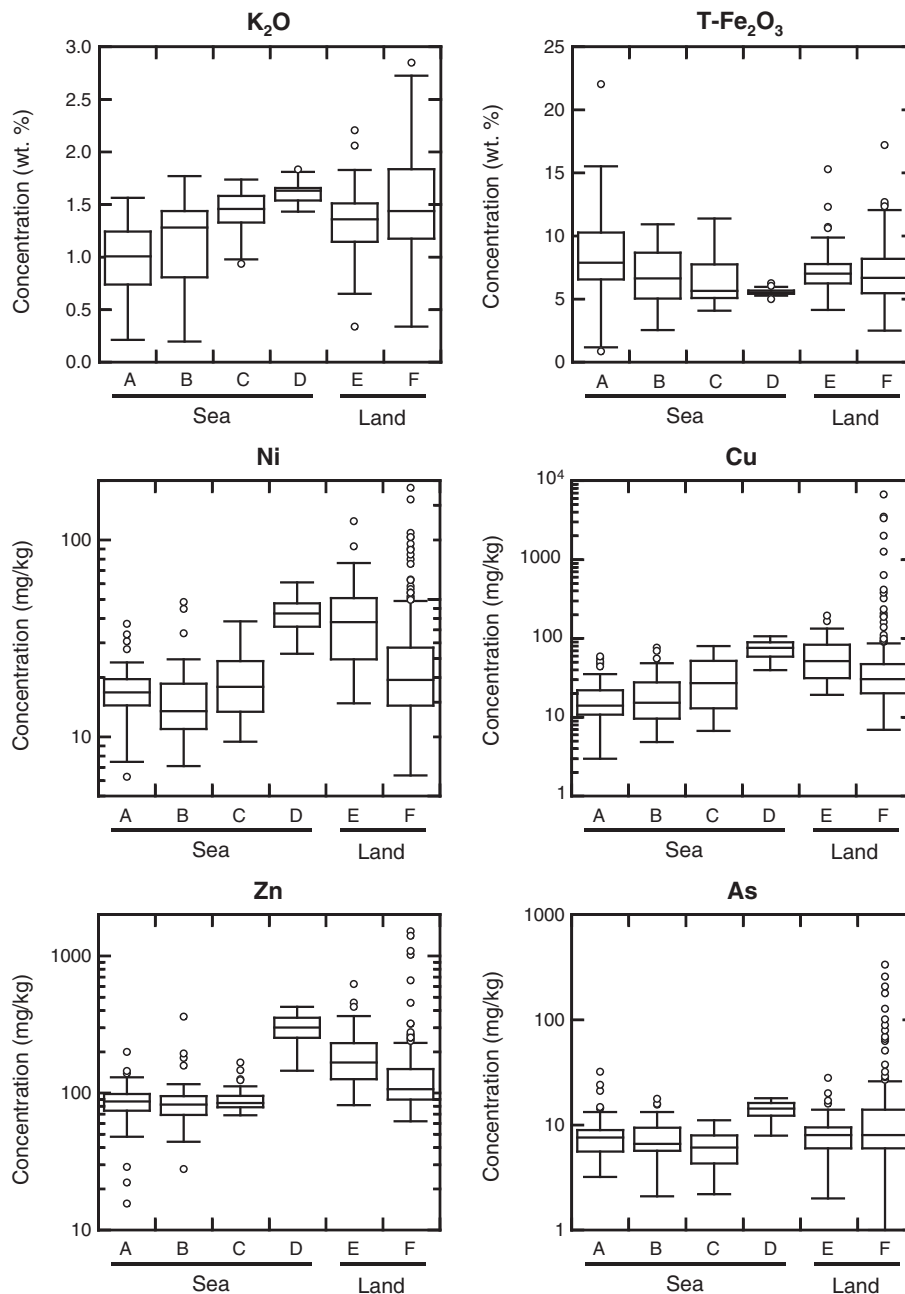


Fig. 5. Box-whisker plots of elemental concentrations in stream and marine sediments. Marine sediment data are subdivided into four groups: (A) gravel-coarse-medium sand; (B) fine-very fine sand; (C) silt in the outer sea, and (D) silt in Tokyo Bay. Stream sediment data are also grouped into sediments from (E) urban area, and (F) from the other regions. The 25th (Q1) and 75th (Q3) percentiles are indicated at the bottom and top of box, respectively. The median is the line across the centre of the box. The higher and lower whisker extends to $Q1 - 1.5 * (Q3 - Q1)$ and $Q3 + 1.5 * (Q3 - Q1)$, respectively. Small circles indicate outliers.

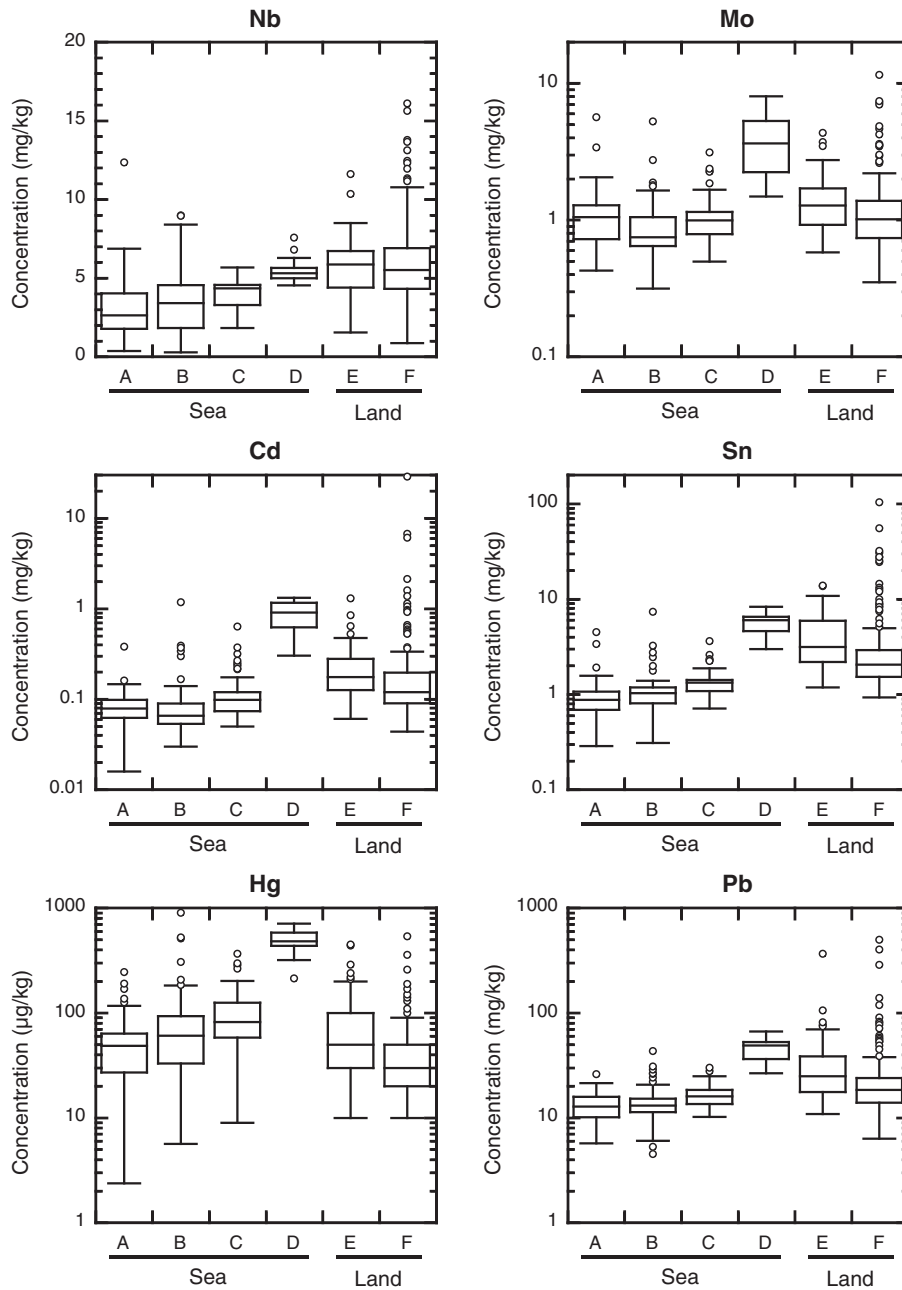


Fig. 5 (continued).

the euripus, and accordingly only coarse sands, including shell fragments, are deposited there. In contrast, the current in both the surface and bottom layers of Tokyo Bay rotates clockwise or anticlockwise, depending on the season, and fine sediments, therefore, remain in the bay in relation to this movement.

The concentration of most elements, including the chalcophile elements, tends to increase with a decrease in sediment grain size because of the dilution effect. Silty sediments are typically found in the deep sea off the Boso Peninsula, and in Sagami Bay. In addition, concentrations of Li, K₂O, Rb, Cs, and Tl are also elevated in both the silty sediments and fine sediments of Tokyo Bay (represented by K₂O in Fig. 4), but these are not influenced by anthropogenic activities.

It was, therefore, examined whether or not the significant enrichment of chalcophile elements was actually a result of anthropogenic activities. Fig. 5 shows a box-and-whisker plot of 12 elements (K₂O, T-Fe₂O₃, Ni, Cu, Zn, As, Nb, Mo, Cd, Sn, Hg, and Pb) from the stream and marine

sediments data sets. The data from marine sediments are grouped into four categories: (A) gravel-coarse-medium sands, (B) fine-very fine sands, (C) silt in Sagami Bay, in the mouth of Tokyo Bay, off Boso Peninsula, and on Kashima-Nada, and (D) silt in Tokyo Bay. The data from stream sediments are further subdivided into two groups: (E) sediments collected from urbanised areas, and (F) other regions. For reference, median concentrations of the 50 elements in sediments are shown in Table 4.

Table 4 shows that the median concentrations of most elements in marine sediments increase with decreasing grain size. In contrast, those of MgO, CaO, MnO, T-Fe₂O₃, Sc, V, and As decrease with decreasing grain size. There are no systematic changes in the median concentrations of Al₂O₃, P₂O₅, TiO₂, Cr, Ni, Zn, and Mo with respect to grain size. Fig. 5 shows that there is no large change in the range of concentrations of the 12 elements in marine sediments.

In order to objectively elucidate the grain size effect and the influence of anthropogenic activity, a one-way analysis of variance

(ANOVA) test and a multiple comparison test were applied to the geochemical data in Table 4. The null hypothesis adopted here was that no significant difference would be found to exist in elemental concentrations among the four groups (A, B, C, and D). The ANOVA result suggests that the null hypothesis is rejected for many elements at the 0.05 confidence level (Table 5). The probabilities of TiO₂, T-Fe₂O₃, V, Co, Y, La, Ce, Nd, Dy, Ho, and Er data obtained by ANOVA are larger than 0.05. This therefore indicates that these elemental concentrations do not differ significantly among the four groups (A, B, C, and D).

The Bonferroni test (a multiple comparison test) was also applied, which can show significant differences in data sets, and as such is a widely used pair-wise comparison method to discriminate between data sets (Ohta et al., 2005). A probability of less than 0.05 indicates a significant difference between data sets. Results of

this show that (see Table 5) gravel and coarse and medium sands (A) have similar elemental concentrations to fine sands (B), except for in concentrations of Al₂O₃, MnO, Ga, Eu, and Hg. In contrast, silty sediments in the outer sea (C) have significantly different concentrations of elements, except for those of P₂O₅, TiO₂, T-Fe₂O₃, V, Cr, Co, Zn, and Nd in samples A and B. These results suggest that the concentration of many elements changes systematically and significantly according to grain size.

Of interest was to discover whether silty sediments in Tokyo Bay (D) have different concentrations in chalcophile elements, Mo, and Sn from the silty sediments in the outer sea (C). It was considered that if there were no existing additional factors, such as contamination from anthropogenic activities, for these elements in Tokyo Bay, the elemental concentrations of samples C and D would be mutually comparable. Results show that the concentrations of 32 elements in the silty sediments

Table 4
Median elemental concentrations of marine and stream sediments, and concentration ratios.

| Elements | Unit | Marine sediment | | | | Stream sediment | | Concentration ratio | |
|----------------------------------|-------|-----------------|------------|------------|------------|-----------------|-------------|---------------------|-----|
| | | A (N = 47) | B (N = 67) | C (N = 57) | D (N = 19) | E (N = 41) | F (N = 179) | D/C | D/F |
| MgO | wt.% | 4.44 | 3.57 | 3.08 | 3.18 | 3.59 | 3.40 | 1.0 | 0.9 |
| Al ₂ O ₃ | wt.% | 9.40 | 10.8 | 10.8 | 8.47 | 10.7 | 10.6 | 0.8 | 0.8 |
| P ₂ O ₅ | wt.% | 0.105 | 0.096 | 0.101 | 0.192 | 0.172 | 0.121 | 1.9 | 1.1 |
| K ₂ O | wt.% | 1.01 | 1.28 | 1.46 | 1.63 | 1.36 | 1.44 | 1.1 | 1.2 |
| CaO | wt.% | 7.64 | 5.94 | 4.39 | 1.58 | 3.13 | 3.04 | 0.4 | 0.5 |
| TiO ₂ | wt.% | 0.66 | 0.59 | 0.61 | 0.57 | 0.74 | 0.76 | 0.9 | 0.8 |
| MnO | wt.% | 0.149 | 0.111 | 0.079 | 0.094 | 0.127 | 0.135 | 1.2 | 0.7 |
| T-Fe ₂ O ₃ | wt.% | 7.89 | 6.65 | 5.67 | 5.55 | 7.03 | 6.69 | 1.0 | 0.8 |
| Li | mg/kg | 17 | 20 | 26 | 51 | 26 | 23 | 2.0 | 2.0 |
| Be | mg/kg | 0.60 | 0.76 | 0.92 | 1.0 | 1.0 | 1.0 | 1.1 | 1.0 |
| Sc | mg/kg | 22 | 18 | 17 | 12 | 17 | 17 | 0.7 | 0.7 |
| V | mg/kg | 148 | 111 | 119 | 110 | 148 | 144 | 0.9 | 0.7 |
| Cr | mg/kg | 41 | 37 | 41 | 98 | 70 | 47 | 2.4 | 1.4 |
| Co | mg/kg | 17 | 14 | 12 | 14 | 19 | 18 | 1.2 | 0.7 |
| Ni | mg/kg | 17 | 14 | 18 | 42 | 38 | 19 | 2.4 | 1.1 |
| Cu | mg/kg | 14 | 15 | 27 | 76 | 51 | 30 | 2.8 | 1.5 |
| Zn | mg/kg | 87 | 82 | 85 | 301 | 167 | 107 | 3.6 | 1.8 |
| Ga | mg/kg | 11 | 13 | 13 | 14 | 15 | 15 | 1.1 | 0.9 |
| As | mg/kg | 6.5 | 6.6 | 6.0 | 14 | 8.0 | 8.0 | 2.4 | 1.8 |
| Rb | mg/kg | 29 | 29 | 32 | 52 | 45 | 49 | 1.6 | 1.2 |
| Sr | mg/kg | 365 | 267 | 204 | 116 | 146 | 143 | 0.6 | 0.8 |
| Y | mg/kg | 13 | 14 | 15 | 14 | 15 | 15 | 0.9 | 0.9 |
| Nb | mg/kg | 2.6 | 3.4 | 4.4 | 5.3 | 5.9 | 5.5 | 1.2 | 0.9 |
| Mo | mg/kg | 1.1 | 0.75 | 1.0 | 3.6 | 1.3 | 1.0 | 3.6 | 2.9 |
| Cd | mg/kg | 0.079 | 0.066 | 0.099 | 0.91 | 0.18 | 0.12 | 9.2 | 5.2 |
| Sn | mg/kg | 0.9 | 1.0 | 1.3 | 6.0 | 3.2 | 2.1 | 4.5 | 1.9 |
| Sb | mg/kg | 0.35 | 0.31 | 0.39 | 0.68 | 0.68 | 0.50 | 1.8 | 1.0 |
| Cs | mg/kg | 1.1 | 1.1 | 1.7 | 3.8 | 2.7 | 2.5 | 2.2 | 1.4 |
| Ba | mg/kg | 193 | 244 | 281 | 206 | 343 | 367 | 0.7 | 0.6 |
| La | mg/kg | 8.6 | 8.8 | 10 | 11 | 14 | 16 | 1.1 | 0.8 |
| Ce | mg/kg | 18 | 18 | 20 | 19 | 24 | 28 | 1.0 | 0.8 |
| Pr | mg/kg | 2.3 | 2.2 | 2.5 | 2.7 | 3.2 | 3.6 | 1.1 | 0.8 |
| Nd | mg/kg | 10 | 9.4 | 10 | 11 | 13 | 14 | 1.1 | 0.9 |
| Sm | mg/kg | 2.1 | 2.2 | 2.5 | 2.5 | 2.7 | 3.0 | 1.0 | 0.9 |
| Eu | mg/kg | 0.60 | 0.67 | 0.69 | 0.64 | 0.73 | 0.75 | 0.9 | 0.9 |
| Gd | mg/kg | 2.2 | 2.3 | 2.4 | 2.5 | 2.6 | 2.8 | 1.0 | 1.0 |
| Tb | mg/kg | 0.39 | 0.41 | 0.46 | 0.46 | 0.47 | 0.49 | 1.0 | 1.0 |
| Dy | mg/kg | 2.1 | 2.2 | 2.5 | 2.4 | 2.5 | 2.5 | 1.0 | 0.9 |
| Ho | mg/kg | 0.43 | 0.45 | 0.49 | 0.46 | 0.51 | 0.49 | 0.9 | 0.9 |
| Er | mg/kg | 1.3 | 1.4 | 1.5 | 1.3 | 1.5 | 1.5 | 0.9 | 0.9 |
| Tm | mg/kg | 0.21 | 0.22 | 0.24 | 0.22 | 0.24 | 0.24 | 0.9 | 0.9 |
| Yb | mg/kg | 1.3 | 1.4 | 1.5 | 1.3 | 1.5 | 1.5 | 0.8 | 0.8 |
| Lu | mg/kg | 0.19 | 0.20 | 0.22 | 0.19 | 0.22 | 0.22 | 0.9 | 0.9 |
| Ta | mg/kg | 0.25 | 0.30 | 0.40 | 0.51 | 0.52 | 0.48 | 1.3 | 1.0 |
| Hg | µg/kg | 49 | 61 | 82 | 483 | 50 | 30 | 5.9 | 9.7 |
| Tl | mg/kg | 0.20 | 0.25 | 0.31 | 0.82 | 0.41 | 0.39 | 2.6 | 2.0 |
| Pb | mg/kg | 13 | 13 | 16 | 49 | 25 | 19 | 3.0 | 2.0 |
| Bi | mg/kg | 0.14 | 0.11 | 0.19 | 0.93 | 0.15 | 0.15 | 4.8 | 6.1 |
| Th | mg/kg | 2.6 | 2.6 | 3.2 | 3.9 | 4.4 | 4.9 | 1.2 | 0.9 |
| U | mg/kg | 0.66 | 0.75 | 0.94 | 1.3 | 1.0 | 1.0 | 1.4 | 1.3 |

A: Gravel and very coarse-coarse-medium sand; B: fine and very fine sand; C: silt in the outer sea; D: silt in the Tokyo Bay; E: stream sediment in urban area; F: stream sediment in the other region.

Table 5
Results of one-way ANOVA and the Bonferroni multiple comparison procedure at the 0.05 confidence interval.

| | P value of ANOVA | Bonferroni multiple comparison test | | | | | |
|----------------------------------|------------------|-------------------------------------|-------------|-------------|-----------------------------------|-------------|-------------|
| | | Particle size comparison | | | Comparison with silt in Tokyo Bay | | |
| | | A:B | A:C | B:C | A:D | B:D | C:D |
| MgO | <0.01 | 0.02 | <0.01 | 0.04 | <0.01 | 0.16 | 0.97 |
| Al ₂ O ₃ | <0.01 | <0.01 | <0.01 | <0.01 | <0.01 | <0.01 | <0.01 |
| P ₂ O ₅ | <0.01 | 0.21 | 0.98 | 0.18 | <0.01 | <0.01 | <0.01 |
| K ₂ O | <0.01 | 0.03 | <0.01 | <0.01 | <0.01 | <0.01 | 0.04 |
| CaO | <0.01 | 0.14 | <0.01 | <0.01 | <0.01 | <0.01 | <0.01 |
| TiO ₂ | 0.95 | 0.60 | 0.65 | 0.96 | 0.98 | 0.72 | 0.75 |
| MnO | <0.01 | <0.01 | <0.01 | <0.01 | 0.02 | 0.75 | 0.05 |
| T-Fe ₂ O ₃ | 0.13 | 0.22 | 0.07 | 0.49 | 0.03 | 0.18 | 0.39 |
| Li | <0.01 | 0.06 | <0.01 | <0.01 | <0.01 | <0.01 | <0.01 |
| Be | <0.01 | 0.01 | <0.01 | <0.01 | <0.01 | <0.01 | <0.01 |
| Sc | <0.01 | 0.13 | <0.01 | 0.12 | <0.01 | <0.01 | 0.01 |
| V | 0.49 | 0.36 | 0.30 | 0.87 | 0.14 | 0.39 | 0.46 |
| Cr | <0.01 | 0.78 | 0.15 | 0.06 | <0.01 | <0.01 | <0.01 |
| Co | 0.10 | 0.20 | 0.01 | 0.16 | 0.42 | 0.94 | 0.30 |
| Ni | <0.01 | 0.05 | 0.17 | <0.01 | <0.01 | <0.01 | <0.01 |
| Cu | <0.01 | 0.97 | <0.01 | <0.01 | <0.01 | <0.01 | <0.01 |
| Zn | <0.01 | 0.80 | 0.19 | 0.24 | <0.01 | <0.01 | <0.01 |
| Ga | <0.01 | <0.01 | <0.01 | <0.01 | <0.01 | <0.01 | 0.10 |
| As | <0.01 | 0.27 | 0.23 | 0.01 | <0.01 | <0.01 | <0.01 |
| Rb | <0.01 | 0.90 | <0.01 | <0.01 | <0.01 | <0.01 | <0.01 |
| Sr | <0.01 | 0.37 | <0.01 | <0.01 | <0.01 | <0.01 | <0.01 |
| Y | 0.05 | 0.53 | <0.01 | 0.03 | 0.65 | 0.99 | 0.14 |
| Nb | <0.01 | 0.41 | <0.01 | 0.03 | <0.01 | <0.01 | <0.01 |
| Mo | <0.01 | 0.04 | 0.85 | 0.04 | <0.01 | <0.01 | <0.01 |
| Cd | <0.01 | 0.72 | <0.01 | <0.01 | <0.01 | <0.01 | <0.01 |
| Sn | <0.01 | 0.19 | <0.01 | <0.01 | <0.01 | <0.01 | <0.01 |
| Sb | <0.01 | 0.04 | <0.01 | <0.01 | <0.01 | <0.01 | <0.01 |
| Cs | <0.01 | 0.72 | <0.01 | <0.01 | <0.01 | <0.01 | <0.01 |
| Ba | <0.01 | 0.46 | <0.01 | <0.01 | 0.22 | 0.46 | 0.01 |
| La | 0.02 | 0.28 | 0.32 | 0.03 | 0.05 | <0.01 | 0.20 |
| Ce | 0.20 | 0.50 | 0.20 | 0.04 | 0.63 | 0.32 | 0.65 |
| Pr | <0.01 | 0.75 | 0.06 | 0.02 | 0.01 | <0.01 | 0.22 |
| Nd | 0.05 | 0.82 | 0.24 | 0.13 | 0.03 | 0.01 | 0.15 |
| Sm | <0.01 | 0.52 | <0.01 | 0.03 | <0.01 | <0.01 | 0.22 |
| Eu | <0.01 | <0.01 | <0.01 | 0.23 | 0.06 | 0.44 | 0.11 |
| Gd | <0.01 | 0.37 | <0.01 | 0.05 | <0.01 | 0.01 | 0.27 |
| Tb | <0.01 | 0.25 | <0.01 | 0.03 | <0.01 | 0.06 | 0.72 |
| Dy | 0.01 | 0.28 | <0.01 | 0.02 | 0.07 | 0.27 | 0.64 |
| Ho | 0.02 | 0.34 | <0.01 | 0.03 | 0.30 | 0.69 | 0.25 |
| Er | 0.01 | 0.37 | <0.01 | 0.01 | 0.58 | 0.94 | 0.08 |
| Tm | <0.01 | 0.43 | <0.01 | 0.01 | 0.93 | 0.62 | 0.03 |
| Yb | <0.01 | 0.52 | <0.01 | <0.01 | 0.75 | 0.42 | 0.01 |
| Lu | <0.01 | 0.55 | <0.01 | <0.01 | 0.56 | 0.30 | <0.01 |
| Ta | <0.01 | 0.41 | <0.01 | <0.01 | <0.01 | <0.01 | <0.01 |
| Hg | <0.01 | <0.01 | <0.01 | 0.01 | <0.01 | <0.01 | <0.01 |
| Tl | <0.01 | 0.49 | <0.01 | <0.01 | <0.01 | <0.01 | <0.01 |
| Pb | <0.01 | 0.27 | <0.01 | <0.01 | <0.01 | <0.01 | <0.01 |
| Bi | <0.01 | 0.09 | <0.01 | <0.01 | <0.01 | <0.01 | <0.01 |
| Th | <0.01 | 0.56 | 0.02 | <0.01 | <0.01 | <0.01 | 0.25 |
| U | <0.01 | 0.55 | <0.01 | <0.01 | <0.01 | <0.01 | 0.01 |

A: Gravel-coarse-medium sand; B: fine-very fine sand; C: silt in the outer sea, D: silt in Tokyo Bay.
A bold-faced type means that the null hypothesis is rejected for $p = 0.05$.

of Tokyo Bay are comparable to those in the outer sea (Table 4). However, the remaining elements are highly enriched in the silty sediment of Tokyo Bay (D), where concentration ratios are greater than 1.5. The Bonferroni test suggests that Li, Be, P₂O₅, Cr, Ni, Cu, Zn, As, Rb, Nb, Mo, Cd, Sn, Sb, Cs, Ta, Hg, Tl, Pb, and Bi concentrations in samples D are significantly higher, and that Al₂O₃, CaO, Sc, Sr, Tm, Yb, and Lu are significantly lower than those in sample C (Table 5).

The significant enrichment of Li, Be, K₂O, Rb, Cs, Ba, and Tl, and the depletion of Al₂O₃, CaO, Sr, Tm, Yb, and Lu in the silt of Tokyo Bay (D) are considered likely to be a reflection of the input of sediments derived from the mélange matrix of local accretionary complexes. Stream sediments derived from this lithology are significantly abundant in alkali elements, Be, and Ba, yet poor in Al₂O₃, CaO, Sc, Sr, and heavy REEs (Ohta et al., 2011). Similarly, it is considered that the enrichment of Cr and Ni

within the sediments of Tokyo Bay (D) may be caused in part by the input of sediment derived from mafic and ultramafic rocks in the accretionary complexes. These elements are transported via the Tama and Ara Rivers to Tokyo Bay (shown by K₂O and Ni in Fig. 4). In contrast, the chalcophile elements, P₂O₅, Mo, and Sn are not highly enriched in the upper river basins. Thus, while the enrichment of Cr, Ni, Cu, Zn, As, Cd, Sn, Sb, Hg, Tl, Pb, and Bi in Tokyo Bay is most likely caused by anthropogenic activity, concentrations of As, Mo, and Bi in the stream sediments from urban areas are not significantly higher than those of other regions (Ohta et al., 2011). This is considered to be attributed to the lack of samples collected from visually polluted stream sediments in this study. Alternatively, it could be attributed to the fact that once these elements are discharged by anthropogenic activities they are dissolved in water, and then subsequently react with silty sediments in the bay.

8. Conclusions

The spatial distribution of 53 elements, including chalcophile elements, in the Kanto region of Japan, was examined. It has been shown how particles that have been influenced by mining and anthropogenic activities are transported from the land to the sea through the local riverine systems and water circulation in the marine environment. Contaminated materials are associated with silty sediments, and are supplied from rivers flowing through urban and industrial areas to Tokyo Bay. However, these sediments remain within the bay and appear to be not dispersed to the outer sea, as a result of estuarine water circulation. In contrast, to the semi-closed environment of Tokyo Bay, the sediments supplied by rivers to the continental shelf are dispersed by wave and coastal sea currents along the Pacific coast.

Acknowledgements

The authors are grateful to Takashi Okai (Geological Survey of Japan, AIST) for his useful suggestions, which helped improve the manuscript and grateful to G. N. Nayak (Goa University, India) and E. Y. Ozkan (Ege University, Turkey) for their thoughtful and careful review of the manuscript.

References

- Aitchison, J., 1986. *The Statistical Analysis of Compositional Data*. Chapman & Hall, London (416 pp.).
- Andersson, M., Carlsson, M., Ladenberger, A., Morris, G., Sadeghi, M., Uhlbäck, J., 2014. *Geochemical Atlas of Sweden*. Geological Survey of Sweden, Elanders Sverige AB (208 pp.).
- Aoyama, M., Tsumune, D., Uematsu, M., Kondo, F., Hamajima, Y., 2012. Temporal variation of Cs-134 and Cs-137 activities in surface water at stations along the coastline near the Fukushima Dai-ichi Nuclear Power Plant accident site, Japan. *Geochem. J.* 46, 321–325.
- Bølviken, B., Bergström, J., Björklund, A., Kontio, M., Lehmspelto, P., Lindholm, T., Magnusson, J., Ottesen, R.T., Steenfelt, A., Volden, T., 1986. *Geochemical Atlas of Northern Fennoscandia*. Geological Surveys of Finland, Norway and Sweden, Helsinki, Trondheim and Stockholm.
- Buccianti, A., 2015. The FOREGS repository: modelling variability in stream waters on a continental scale revising classical diagrams from CoDA (compositional data analysis) perspective. In: Demetriades, A., Birke, M., Albanese, S., Schoeters, I., De Vivo, B. (Eds.), *Continental, Regional and Local Scale Geochemical Mapping*. Special Issue, Journal of Geochemical Exploration (in this issue).
- Buckley, D.E., Winters, G.V., 1992. Geochemical characteristics of contaminated surficial sediments in Halifax Harbor – impact of waste discharge. *Can. J. Earth Sci.* 29, 2617–2639.
- Caritat, P., de Cooper, M., 2011a. National Geochemical Survey of Australia: data quality assessment. *Geoscience Australia Record 2011/21* (478 pp., http://www.ga.gov.au/corporate_data/71971/Rec2011_021_Vol1.pdf).
- Caritat, P., de Cooper, M., 2011b. National Geochemical Survey of Australia: the geochemical atlas of Australia. *Geoscience Australia Record 2011/20* (557 pp., http://www.ga.gov.au/corporate_data/71971/Rec2011_021_Vol2.pdf).
- Chandrajith, R., Dissanayake, C.B., Tobschall, H.J., 2000. Sources of stream sediments in the granulite terrain of the Walawe Ganga Basin, Sri Lanka, indicated by rare earth element geochemistry. *Appl. Geochem.* 15, 1369–1381.
- Chandrajith, R., Dissanayake, C.B., Tobschall, H.J., 2001. Application of multi-element relationships in stream sediments to mineral exploration: a case study of Walawe Ganga Basin, Sri Lanka. *Appl. Geochem.* 16, 339–350.
- Cicchella, D., De Vivo, B., Lima, A., Albanese, S., Fedele, L., 2008. Urban geochemical mapping in the Campania region (Italy). *Geochem. Explor. Environ. Anal.* 8, 19–29.
- Darnley, A.G., Björklund, A., Bølviken, B., Gustavsson, N., Koval, P.V., Plant, J.A., Steenfelt, A., Tauchid, M., Xie, X., Garrett, R.G., Hall, G.E.M., 1995. A global geochemical database for environmental and resource management: recommendations for international geochemical mapping. UNESCO Publishing, Paris (122 pp., http://www.globalgeochemicalbaselines.eu/wp-content/uploads/2012/07/Blue_Book_GGD_JGCP259.pdf).
- De Vos, W., Tarvainen, T. (Chief Eds.), Salminen, R., Reeder, S., De Vivo, B., Demetriades, A., Piric, S., Batista, M.J., Marsina, K., Ottesen, R.-T., O'Connor, P.J., Bidovec, M., Lima, A., Siewers, U., Smith, B., Taylor, H., Shaw, R., Salpeteur, I., Gregorauskiene, V., Halamic, J., Slaninka, I., Lax, K., Gravesen, P., Birke, M., Breward, N., Ander, E.L., Jordan, G., Duris, M., Klein, P., Locutura, J., Bel-lan, A., Pasieczna, A., Lis, J., Mazreku, A., Gilucis, A., Heitzmann, P., Klaver, G., Petersell, V., 2006. *Geochemical atlas of Europe. Part 2 – interpretation of geochemical maps, additional tables, figures, maps, and related publications*. Geological Survey of Finland, Espoo, Finland, 692 pp., <http://weppi.gtk.fi/publ/foregsatlas/>
- Egozcue, J.J., Pawłowsky-Glahn, V., 2011. Basic concepts and procedures. Chapter 2. In: *Pawłowsky-Glahn, V., Buccianti, A. (Eds.), Compositional Data Analysis: Theory and Applications*. John Wiley & Sons Ltd, Chichester, U.K., pp. 12–28.
- Fang, T.H., Li, J.Y., Feng, H.M., Chen, H.Y., 2009. Distribution and contamination of trace metals in surface sediments of the East China Sea. *Mar. Environ. Res.* 68, 178–187.
- Fauth, H., Hindel, R., Siewers, U., Zinner, J., 1985. *Geochemischer Atlas Bundesrepublik Deutschland*. Bundesanstalt für Geowissenschaften und Rohstoffe (BGR), Hannover (in German) (79 pp.).
- Filzmoser, P., Hron, K., Reimann, C., 2009. Univariate statistical analysis of environmental (compositional) data – problems and possibilities. *Sci. Total Environ.* 407, 6100–6108.
- Filzmoser, P., Hron, K., Reimann, C., 2010. The bivariate statistical analysis of environmental (compositional) data. *Sci. Total Environ.* 408, 4230–4238.
- Filzmoser, P., Reimann, C., Birke, M., 2014. Univariate data analysis and mapping. Chapter 8. In: Reimann, C., Birke, M., Demetriades, A., Filzmoser, P., O'Connor, P. (Eds.), *Chemistry of Europe's Agricultural Soils – Part A*. Geologisches Jahrbuch (Reihe B102), Schweizerbart, Hannover, pp. 67–81.
- Geological Survey of Japan, 1992. *Geological Map of Japan, 1:1,000,000 (3rd, Ed.)*. Tsukuba.
- Gustavsson, N., Bølviken, B., Smith, D.B., Severson, R.C., 2001. *Geochemical landscapes of the conterminous United States: new map presentations for 22 elements*. US Geol. Surv. Prof. Pap. 1648, 1–38.
- Hawkes, H.E., 1957. *Principles of geochemical prospecting*. U.S. Geol. Surv. Bull. 100-F, 225–355.
- Hawkes, H.E., Webb, J.S., 1962. *Geochemistry in Mineral Exploration*. Harper & Row, Publishers, New York (415 pp.).
- Higashi, H., Maki, H., 2008. A quasi-3D numerical simulation for hydrodynamic circulation in Tokyo Bay using CIP-FEM. *Proc. Hydraul. Eng.* 52, 1405–1410 (in Japanese with English abstract).
- Howarth, R.J., Thornton, I., 1983. *Regional geochemical mapping and its application to environmental studies*. In: Thornton, I. (Ed.), *Applied Environmental Geochemistry*. Academic Press, London, pp. 41–73.
- Imai, N., 1990. Multielement analysis of rocks with the use of geological certified reference material by inductively coupled plasma mass spectrometry. *Anal. Sci.* 6, 389–395.
- Imai, N., Terashima, S., Itoh, S., Ando, A., 1995. 1994 compilation of analytical data for minor and trace-elements in 17 GSJ geochemical reference samples, igneous rock series. *Geostand. Newslett.* 19, 135–213.
- Imai, N., Terashima, S., Ohta, A., Mikoshihara, M., Okai, T., Tachibana, Y., Togashi, S., Matsuhiwa, Y., Kanai, Y., Kamioka, H., Taniguchi, M., 2004. *Geochemical map of Japan*. Geological Survey of Japan, AIST, Tsukuba 1st ed. (available from <https://gbank.gsj.jp/geochemmap/> [Accessed: 29 October 2014]).
- Imai, N., Terashima, S., Ohta, A., Mikoshihara, M., Okai, T., Tachibana, Y., Togashi, S., Matsuhiwa, Y., Kanai, Y., Kamioka, H., 2010. *Elemental distribution in Japan – geochemical map of Japan*. In: Imai, N. (Ed.), *Geological Survey of Japan, AIST, Tsukuba* (available from <https://gbank.gsj.jp/geochemmap/> [Accessed: 29 October 2014]).
- Jarva, J., Tarvainen, T., Reinikainen, J., 2008. Application of arsenic baselines in the assessment of soil contamination in Finland. *Environ. Geochem. Health* 30, 613–621.
- Johnson, C.C., Ander, E.L., 2008. Urban geochemical mapping studies: how and why we do them. *Environ. Geochem. Health* 30, 511–530.
- Johnson, C.C., Demetriades, A., Locutura, J., Ottesen, R.T. (Eds.), 2011. *Mapping the Chemical Environment of Urban Areas*. John Wiley & Sons Ltd, Chichester, U.K. (616 pp.).
- Koljonen, T., 1992. *The Geochemical Atlas of Finland, Part 2: Till*. Geological Survey of Finland, Espoo, Finland (212 pp.).
- Kubo, J., 1989. Natural condition in southern Tokiwa region and Kashima-Nada. *Research Paper of Ibaraki Prefecture Fisheries Experimental Station* 27 pp. 1–26 (in Japanese).
- Lahermo, P., Ilmasti, M., Juntunen, R., Taka, M., 1990. *The Geochemical Atlas of Finland, Part 1: The Hydrogeochemical Mapping of Finnish Groundwater*. Geological Survey of Finland, Espoo (66 pp.).
- Lahermo, P., Väänänen, P., Tarvainen, T., Salminen, R., 1996. *Geochemical atlas of Finland. Part 3: Environmental Geochemistry – Stream Waters and Sediments*. Geological Survey of Finland, Espoo (149 pp.).
- Leoni, L., Sartori, F., 1996. Heavy metals and arsenic in sediments from the continental shelf of the northern Tyrrhenian eastern Ligurian seas. *Mar. Environ. Res.* 41, 73–98.
- Levinson, A.A., 1974. *Introduction to Exploration Geochemistry*. Applied Publishing Ltd., Wilmette, Illinois, USA (614 pp.).
- Levinson, A.A., 1980. *Introduction to Exploration Geochemistry*. Applied Publishing Ltd., Wilmette, Illinois, U.S.A. (924 pp.).
- Li, X.D., Shen, Z.G., Wai, O.W.H., Li, Y.S., 2001. Chemical forms of Pb, Zn and Cu in the sediment profiles of the Pearl River Estuary. *Mar. Pollut. Bull.* 42, 215–223.
- Li, X.D., Lee, S.L., Wong, S.C., Shi, W.Z., Thornton, L., 2004. The study of metal contamination in urban soils of Hong Kong using a GIS-based approach. *Environ. Pollut.* 129, 113–124.
- Lis, J., Pasieczna, A., 1995. *Geochemical Atlas of Poland 1: 2500000*. Polish Geological Institute, Warszawa.
- Mogi, A., 1970. Topography of the continental shelf. *Kaiyo Kagaku* 2, 23–28 (in Japanese with English abstract).
- Ohta, A., Imai, N., 2011. Comprehensive survey of multi-elements in coastal sea and stream sediments in the island arc region of Japan: mass transfer from terrestrial to marine environments. In: El-Amin, M. (Ed.), *Advanced Topics in Mass Transfer*. InTech, Croatia, pp. 373–398.
- Ohta, A., Imai, N., Terashima, S., Tachibana, Y., Ikehara, K., Nakajima, T., 2004. *Geochemical mapping in Hokuriku, Japan: influence of surface geology, mineral occurrences and mass movement from terrestrial to marine environments*. *Appl. Geochem.* 19, 1453–1469.
- Ohta, A., Imai, N., Terashima, S., Tachibana, Y., 2005. Application of multi-element statistical analysis for regional geochemical mapping in Central Japan. *Appl. Geochem.* 20, 1017–1037.
- Ohta, A., Imai, N., Terashima, S., Tachibana, Y., Ikehara, K., Okai, T., Ujiie-Mikoshihara, M., Kubota, R., 2007. Elemental distribution of coastal sea and stream sediments in the island-arc region of Japan and mass transfer processes from terrestrial to marine environments. *Appl. Geochem.* 22, 2872–2891.
- Ohta, A., Imai, N., Terashima, S., Tachibana, Y., Ikehara, K., Katayama, H., Noda, A., 2010. Factors controlling regional spatial distribution of 53 elements in coastal sea

- sediments in northern Japan: comparison of geochemical data derived from stream and marine sediments. *Appl. Geochem.* 25, 357–376.
- Ohta, A., Imai, N., Terashima, S., Tachibana, Y., 2011. Regional geochemical mapping in eastern Japan including the nation's capital, Tokyo. *Geochem. Explor. Environ. Anal.* 11, 211–223.
- Omori, M., Hayama, Y., Horiguchi, M., 1986. *Regional Geology of Japan. Part 3 (KANTO)*. Kyoritsu Shuppan Co (in Japanese).
- Reimann, C., 2005. Geochemical mapping: technique or art? *Geochem. Explor. Environ. Anal.* 5, 359–370.
- Reimann, C., Filzmoser, P., Garrett, R.G., 2002. Factor analysis applied to regional geochemical data: problems and possibilities. *Appl. Geochem.* 17, 185–206.
- Reimann, C., Siewers, U., Tarvainen, T., Bitukova, L., Eriksson, J., Gilucis, A., Gregorauskiene, V., Lukashev, V., Matinian, N., Pasieczna, A., 2003. *Agricultural Soils in Northern Europe: A Geochemical Atlas*. E. Schweizerbart'sche Verlagsbuchhandlung, Stuttgart, Germany.
- Reimann, C., Filzmoser, P., Fabian, K., Hron, K., Birke, M., Demetriades, A., Dinelli, E., Ladenberger, A., The GEMAS Project Team, 2012. The concept of compositional data analysis in practice – total major element concentrations in agricultural and grazing land soils of Europe. *Sci. Total Environ.* 426, 196–210.
- Reimann, C., Birke, M., Demetriades, A., Filzmoser, P., O'Connor, P., 2014a. Chemistry of Europe's Agricultural Soils – Part A: Methodology and Interpretation of the GEMAS Data Set. *Geologisches Jahrbuch (Reihe B 102)*, Schweizerbarth, Hannover (528 pp.).
- Reimann, C., Birke, M., Demetriades, A., Filzmoser, P., 2014b. Chemistry of Europe's Agricultural Soils – Part B: General Background Information and Further Analysis of the GEMAS Data Set. In: O'Connor, P. (Ed.), *Geologisches Jahrbuch (Reihe B 103)*, Schweizerbarth, Hannover (352 pp.).
- Rose, A.W., Hawkes, H.E., Webb, J.S., 1979. *Geochemistry in Mineral Exploration*. Academic Press, London (657 pp.).
- Sadeghi, M., Billay, A., Carranza, E.J.M., 2015. Analysis and mapping of soil geochemical anomalies: implications for bedrock mapping and gold exploration in Giyani area, South Africa. In: Demetriades, A., Birke, M., Albanese, S., Schoeters, I., De Vivo, B. (Eds.), *Continental, Regional and Local Scale Geochemical Mapping*. Special Issue, *Journal of Geochemical Exploration* (in this issue).
- Salminen, R. (Chief Ed.), Batista, M.J., Bidovec, M., Demetriades, A., B., D.V., De Vos, W., Duris, M., Gilucis, A., Gregorauskiene, V., Halamic, J., Heitzmann, P., Lima, A., Jordan, G., Klaver, G., Klein, P., Lis, J., Locutura, J., Marsina, K., Mazreku, A., O'Connor, P.J., Olsson, S.Å., Ottesen, R.-T., Petersell, V., Plant, J.A., Reeder, S., Salpeteur, I., Sandström, H., Siewers, U., Steenfelt, A., Tarvainen, T., 2005. *Geochemical atlas of Europe. Part 1 – background information, methodology and maps*. Geological Survey of Finland, Espoo, Finland, 526 pp., <http://weppi.gtk.fi/publ/foregsatlas/>
- Shacklette, H.T., Boerngen, J.G., 1984. *Element Concentrations in Soils and Other Surficial Materials of the Conterminous United States*. United States Government Printing Office.
- Shapiro, S.S., Wilk, M.B., 1965. An analysis of variance test for normality (complete samples). *Biometrika* 52, 591–611.
- Smith, D.B., Cannon, W.F., Woodruff, L.G., Solano, F., Kilburn, J.E., Fey, D.L., 2013. Geochemical and mineralogical data for soils of the conterminous United States. U.S. Geol. Surv. Data Ser. 801 (19 pp., <http://pubs.usgs.gov/ds/801/>).
- Smith, D.B., Cannon, W.F., Woodruff, L.G., Solano, F., Ellefsen, K.J., 2014. Geochemical and mineralogical maps for soils of the conterminous United States. U.S. Geological Survey Open-File Report 2014-1082 (386 pp., <http://pubs.usgs.gov/of/2014/1082/pdf/ofr2014-1082.pdf>).
- Thalman, F., Schermann, O., Schroll, E., Hausberger, G., 1989. *Geochemical atlas of the Republic of Austria 1:1,000,000, Bohemian massif and central zone of the Eastern Alps (stream sediments <80 mesh)*. Geological Survey of Austria.
- Thornton, I., Farago, M.E., Thums, C.R., Parrish, R.R., McGill, R.A.R., Breward, N., Fortey, N.J., Simpson, P., Young, S.D., Tye, A.M., Crout, N.M.J., Hough, R.L., Watt, J., 2008. Urban geochemistry: research strategies to assist risk assessment and remediation of brownfield sites in urban areas. *Environ. Geochem. Health* 30, 565–576.
- Watson, D.F., Philip, G.M., 1985. A refinement of inverse distance weighted interpolation. *Geo-Processing* 2, 315–327.
- Weaver, T.A., Broxton, D.E., Bolivar, S.L., Freeman, S.H., 1983. *The Geochemical Atlas of Alaska: Compiled by the Geochemistry Group, Earth Sciences Division*. Los Alamos National Laboratory, Los Alamos (GJBX-32(83)).
- Webb, J.S., Thornton, I., Thompson, M., Howarth, R.J., Lowenstein, P.L., 1978. *The Wolfson Geochemical Atlas of England and Wales*. Clarendon Press, Oxford.
- Whalley, C., Rowlett, S., Bennett, M., Lovell, D., 1999. Total arsenic in sediments from the western North Sea and the Humber Estuary. *Mar. Pollut. Bull.* 38, 394–400.
- Xie, X.J., Mu, X.Z., Ren, T.X., 1997. Geochemical mapping in China. *J. Geochem. Explor.* 60, 99–113.
- Zheng, C., 1994. *Atlas of Soil Environmental Background Value in the People's Republic of China*. China Environmental Science Press, Beijing.